Journal of Hazardous Materials 476 (2024) 135044

Contents lists available at ScienceDirect

Journal of Hazardous Materials

journal homepage: www.elsevier.com/locate/jhazmat

Long-term tracking of the microbiology of uranium-amended water-saturated bentonite microcosms: A mechanistic characterization of U speciation

Mar Morales-Hidalgo [a,*], Cristina Povedano-Priego [a], Marcos F. Martinez-Moreno [a], Jesus J. Ojeda [b], Fadwa Jroundi [a], Mohamed L. Merroun [a]

[a] Faculty of Science, Department of Microbiology, University of Granada, Granada, Spain
[b] Department of Chemical Engineering, Faculty of Science and Engineering, Swansea University, Swansea, United Kingdom

HIGHLIGHTS

- U long-term amendment shaped the bentonite microbial communities.
- Viable sulfate-reducing bacteria like *Desulfovibrio* were enriched.
- U is present as U(VI) and U(IV) species in the full-saturated bentonite microcosm.
- Biogenic uraninite, U(VI) phosphates and U(VI)-adsorbed to clays were identified.

GRAPHICAL ABSTRACT

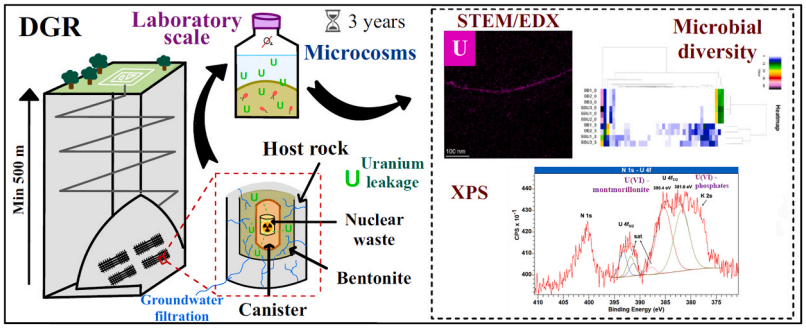

ARTICLE INFO

Keywords:
DGR
Bentonite slurry
Uranium
Long-term incubation
Microbial diversity
Sulfate-reducing bacteria

ABSTRACT

Deep geological repositories (DGRs) stand out as one of the optimal options for managing high-level radioactive waste (HLW) such as uranium (U) in the near future. Here, we provide novel insights into microbial behavior in the DGR bentonite barrier, addressing potential worst-case scenarios such as waste leakage (e.g., U) and groundwater infiltration of electron rich donors in the bentonite. After a three-year anaerobic incubation, Illumina sequencing results revealed a bacterial diversity dominated by anaerobic and spore-forming microorganisms mainly from the phylum Firmicutes. Highly U tolerant and viable bacterial isolates from the genera *Peribacillus*, *Bacillus*, and some SRB such as *Desulfovibrio* and *Desulfosporosinus*, were enriched from U-amended bentonite. The results obtained by XPS and XRD showed that U was present as U(VI) and as U(IV) species. Regarding U(VI), we have identified biogenic U(VI) phosphates, $U(UO_2)\cdot(PO_4)_2$, located in the inner part of the bacterial cell membranes in addition to U(VI)-adsorbed to clays such as montmorillonite. Biogenic U(IV) species as uraninite may be produced as result of bacterial enzymatic U(VI) reduction. These findings suggest that under electron donor-rich water-saturation conditions, bentonite microbial community can control U speciation, immobilizing it, and thus enhancing future DGR safety if container rupture and waste leakage occurs.

* Corresponding author.
E-mail address: marmh@ugr.es (M. Morales-Hidalgo).

https://doi.org/10.1016/j.jhazmat.2024.135044
Received 5 March 2024; Received in revised form 14 June 2024; Accepted 25 June 2024
Available online 26 June 2024

1. Introduction

Nuclear energy is currently gaining global attention for the production of electricity with no greenhouse gas emissions to combat climate change [1]. The main challenge associated with nuclear energy is the proper and safer disposal of radioactive waste. Since 1980, the United Nations have the commitment to protect future generations from the damage related to these types of residues. Over the past few decades, several approaches have been proposed to manage high-level radioactive waste (HLW). Deep geological repositories (DGRs) have emerged as the internationally preferred and safest option for the final disposal of the HLW, as a result of intensive investigation in this area that have lasted for over forty years [2]. DGR consists of a multi-barrier system composed of geological (host rock) and geo-technical barriers (metal canisters and filling/sealing materials) placed at a depth of few hundred meters[3]. Upon closure, the repository environment will undergo a transition process from relatively short initial oxic phase of about 100 years to stable reducing conditions due to factors such as low sub-surface oxygen, microbial metabolism, and mineral dissolution [4]. Several countries such as Finland, Sweden, Switzerland, France, and Spain have selected bentonite as the most suitable backfilling and sealing material, since it serves to seal up the DGR upon saturation with groundwater [5, 6]. Moreover, the bentonite barrier is also very important since it could act as a radionuclide sorbent retarding, thus, their migration in case of a leakage [7]. As far as Spain is concerned, bentonite from "El Cortijo de Archidona" located in Almeria has been extensively studied and its use is currently being considered by the ENRESA company (Empresa Nacional de Residuos Radiactivos, S.A.) as the preferred sealing material for future Spanish DGRs [8]. Microorganisms are able to inhabit and influence all types of environments on Earth, including future DGRs. Several research studies have reported the high microbial diversity in bentonites including the Spanish one [9–13]. This microbial diversity will include autochthonous microorganisms and those accidentally introduced during the construction of the repository. For example, anaerobic bacterial groups such as sulfate-reducing (SRB) and iron-reducing bacteria (IRB), can potentially be active under DGR conditions and cause corrosion in future metallic canisters, as well as induce changes in the mineralogy of the backfill and sealing material [14-16]. Therefore, the study of both the diversity of microorganisms and their metabolic activity is crucial to evaluate the safety performance of HLW repositories during their lifespan (up to 100,000 years depending on the model) [17]. It is well-documented that microbes can interact with heavy metals, including the most critical and principally stored radionuclides, i.e. uranium, through several mechanisms such as bioaccumulation, biosorption, biotransformation or biomineralization [18-22]. In the case of a breakdown in the multi-barrier disposal system, uranium has the potential to migrate through rock fractures and groundwater, eventually finding its way into the biosphere. The two main oxidation states of U are U(VI), as the oxidized form, and U(IV), as the reduced one. U(VI) possess higher solubility and, therefore, higher toxicity to the microbial cells compared to U(IV) [23]. Lopez-Fernandez et al. [11] showed that, in the case of Spanish bentonite, the presence of uranium enriches U-tolerant bacterial strains from the phyla Proteobacteria, Firmicutes, and Actinobacteria. In the same study, isolated strains such as *Arthrobacter, Pseudomonas, Sphingomonas* and *Micrococcus* tolerated a minimum of 2 mM of uranyl nitrate. It is also well-known that SRB are present in bentonites, where they may play a critical role in the biogeochemical cycle of uranium [14,24].

Previous studies have focused on assessing the effect of uranium on the microbial community of unsaturated bentonite, reporting the enrichment of genera such as *Clostridium*, *Sulfurimonas*, *Desulfovibrio* and *Pseudomonas* [13,25,26]. However, little is known about this uranium effect in a water-saturated environment. Therefore, we have aimed to take a few steps further in our study by simulating one of the worst scenarios that could occur in a repository: total filtration of groundwater (super-saturation), the presence of electron donors (such as sodium acetate), uranium leakage (such as uranyl acetate) and micro organism activity (by inoculation of a specific bacterial consortium). Povedano-Priego et al. [27] studied similar conditions in their research, but in the presence of selenium. Furthermore, to the best of our knowledge, this is the first time that the impact of long-term incubation (3 years) has been studied in bentonite slurries. Therefore, we have aimed to firstly investigate alterations in the microbiology of bentonite following a 3-year exposure to uranium, with a specific focus on assessing the viability of heterotrophic microorganisms and sulfate-reducing bacteria, and secondly examine changes in the chemical speciation of uranium over the incubation time, aiming to understand the evolving dynamics influenced by the microbial communities within the bentonite.

2. Material and methods

2.1. Experimental set up and elaboration of the microcosms

Spanish bentonite from "El Cortijo de Archidona" (Almería, Spain) was collected at approximately 90 cm deep in sterile containers using a soil auger under aseptic conditions. Once in the laboratory, the bentonite was stored at 4 °C until further use.

The microcosms were prepared according to the detailed protocol described in Povedano-Priego et al., [27]. Briefly, bentonite was previously dried at room temperature (approximately 25 °C) and homogenized inside a laminar flow hood. Each 250 mL sterile borosilicate bottle contained 40 g of ground bentonite saturated with 170 mL of equilibrium water, which was obtained by mixing 1 g of bentonite with 100 mL of distilled water for 24 h at 180 rpm. Then, the supernatant was collected after centrifuging at 10,000 x g for 5 min and sterilized by autoclave. The major elements composition of the equilibrium water was determined by Inductively Coupled Plasma-Mass Spectroscopy (ICP-MS) with a NexION 300D spectrometer. The data is provided in Supplementary Table S1. The pH (8.51 ± 0.15), oxidation-reduction potential (136.5 ± 1.06 eV) and conductivity (161.63 ± 0.49 μS/cm) were also measured in triplicate using a multi-parameter probe HQd Field Case HACH. The pH values of all the treatments were also analyzed in triplicate before (T. 0) and after 3, 6, and 9 months, and 3 years of incubation following the same methodology.

To accelerate the microbial processes, the microcosms were amended with electron donors such as sodium acetate (30 mM) and glycerol-2-phosphate (G2P, 10 mM), with each microcosm reaching a final volume of 230 mL. Furthermore, G2P was added as a carbon and organic phosphate source. Microcosms corresponding to uranium treatments (U) contained a final concentration of 1.26 mM uranyl acetate ($C_4H_6O_6U$) to study its effect on bentonite microbial diversity. This low concentration of uranium has been selected to simulate the initial stages of a progressive filtration of an uranium leak from the metal canister to the bentonite barrier. A stock solution of uranyl acetate (1 M) was prepared by dissolving the correct amount of the metal salt in $NaClO_4$ solution at 0.1 M. $NaClO_4$ was used to prepare the uranium stock solution due to its high solubility in water contributing to the solubility of uranyl acetate in comparison to other salts. In addition, it is relatively inert, which would prevent reactions and the formation of complexes with other compounds. The stock solution was sterilized by filtration through 0.22 μm nitrocellulose filters since uranium solution cannot be autoclaved to avoid abiotic precipitation of this heavy metal at high temperatures. Subsequently the solution was stored at 4 °C until further use.

Moreover, some microcosms were inoculated with a bacterial consortium (BB) composed of 4 genera, previously identified in other studies to belong to the bacterial community of the Spanish bentonite [11,13,16,25]. The strains *Bacillus* sp. BII-C3 and *Stenotrophomonas bentonitica* BII-R7 have been isolated from the Spanish bentonite, whilst *Pseudomonas putida* ATCC33015 and *Amycolatopsis ruanii* NCIMB14711 were purchased from the culture collection ATCC (American Type Culture Collection; https://www.lgcstandardsatcc.org/) and NCIMB

(National Collection of Industrial Food and Marine Bacteria; https://www.ncimb.com/), respectively. *Bacillus* sp. BII-C3, *S. bentonitica* BII-R7 and *P. putida* were incubated in lysogenic broth (LB), whilst *A. ruanni* was grown in yeast-malt-glucose (YMG) medium. After the incubation time (48 h at 28 °C and 180 rpm.), the cells were harvested (at 10,000 x g for 5 min) and washed twice with sodium chloride 0.9 %, and one last time with the equilibrium water. The microcosms were inoculated with each strain at a final optical density of 0.4 (measured at 600 nm) (Genesys 10 S UV-Vis; Thermo scientific, MA, USA).

Relevant conditions for the future DGRs were decided for the sample incubation: anoxia, darkness, and room temperature. The anoxic atmosphere was established using an inflow of N_2 for 20 min through butyl-rubber stopper. Three replicates of each treatment were elaborated (a total of 6 microcosms) (Fig. 1). Bentonite, interface, and supernatant samples were collected before (T_0) and after 3- year incubation (T_3). Natural bentonite (NB) from the field without any treatment has also been studied.

2.2. Microbial diversity analyses

2.2.1. DNA extraction from bentonite samples

The microbial diversity of each treatment was studied by Next-Generation Sequencing (NGS). Firstly, DNA extractions of the bentonite microcosm samples were performed according to the phenol-chloroform-based protocol described in detail by Povedano-Priego et al. [16]. The mechanical lysis was carried out by mixing sterile glass beads with approximately 400 μL of bentonite slurry in 2 mL screw-tubes. 400 mL of NaH_2PO_4 solution (0.12 M, pH 8), 500 mL of lysis buffer, and 24 μL of freshly made lysozyme, as well as 2 μL of proteinase K were added to perform the chemical lysis. The phenol-chloroform washing steps separate the DNA from the rest of the cellular debris. Subsequently, isopropanol and sodium acetate precipitate the DNA, which is then purified from impurities using 80 % ethanol. The concentrations of the obtained DNA were measured by Qubit 3.0 Fluorometer (Life Technology, Invitrogen™).

2.2.2. Extracted DNA amplification and sequencing

For the total community analysis, 16S rRNA gene libraries were constructed and sequenced by StabVida Company (Caparica, Portugal, https://www.stabvida.com/es). Specifically, V3-V4 variable regions of the bacterial 16S rRNA gene were amplified by PCR using the universal primers 341F (5′-CCTACGGGNGGCWGCAG-3′) and 785R (5′-GACTACHVGGGTATCTAATCC-3′) [28].

Prior to amplifications, the samples were subjected to a quality control to guarantee good DNA integrity. The DNA was then purified using Sera-Mag Select kit (Cytiva) and the libraries were sequenced using MiSeq Reagent Kit v3 and 300 bp paired end with the Illumina MiSeq platform.

2.2.3. Bioinformatics and statistical analysis

Sequencing data were processed and analyzed using QIIME2 v2022.2 [29]. The raw data were denoised using DADA2 plugin as to remove low-quality regions, dereplicate the reads, and filter the chimeras [30].

Alpha rarefaction curves were performed to check the quality of sequencing. After verification, the reads were grouped into OTUs and classified by taxon according to SILVA database (release 138 QIIME), with a clustering threshold of 99 % similarity. Relative abundances of the taxa and alpha diversity indices were obtained using Explicet 2.10.5 [31]. A heatmap was created to represent differences between the bentonite treatments considering only genera with ≥ 1 % relative abundance, by using the heatmap.2 function (gplots v. 3.0.1.1, "phyloseq", and "RColorBrewer" package) of R v.4.2.1 software [32-35]. In addition, a principal coordinate analysis (PCoA) was performed using Past 4.04 [36] software based on the Bray-Curtis algorithm. Raw data were deposited in the Sequence Read Archive (SRA) at the National Center for Biotechnology Information (NCBI) under the Bio-Project ID number PRJNA1083466.

2.3. Survival of bacterial cells after incubation time

2.3.1. Heterotrophic aerobe survival and isolation of the selected strains

After 3-years of incubation (T_3), the heterotrophic aerobes were enumerated in triplicate using lysogenic broth (LB) agar medium at 10 %. The number of viable cells was obtained as colony-forming units (CFU). For this purpose, 0.5 g of bentonite slurry with the bacterial consortium inoculated, with (T3_BBU) and without U (T3_BB), were re-suspended in 4.5 mL of sodium chloride 0.9 % and the suspensions were stirred for 24 h at 128 rpm. Decimal dilutions were then prepared (to dilution 10^{-5}) and used to inoculate plates of 10 % LB agar medium in triplicate, which were incubated for 72 h at 28 °C.

From the T3_BBU treatment, those colonies with different morphologies and colour were isolated and purified in LB 10 % medium, since

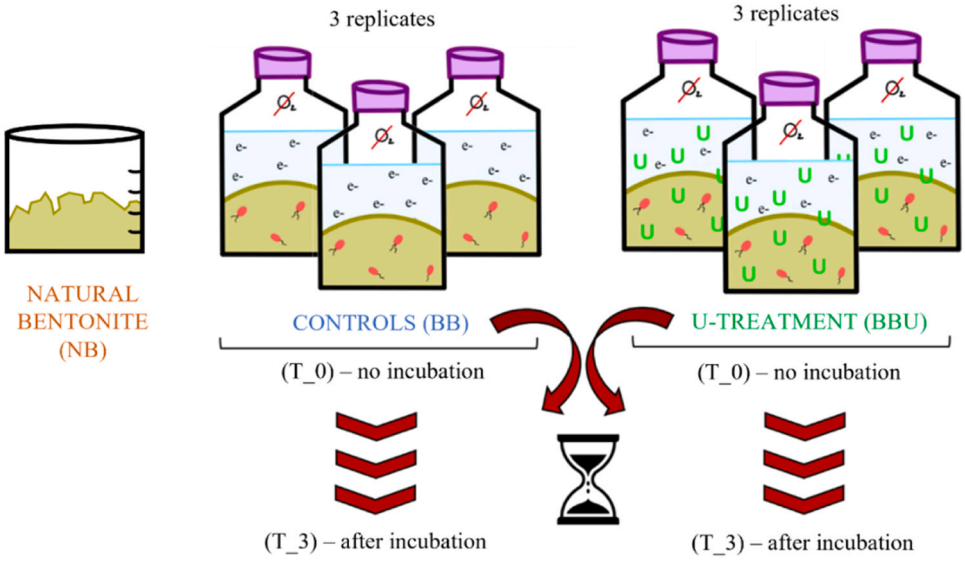

Fig. 1. Schematic composition of the water-saturated microcosms under study (both controls and U-treated) incubated for 3 years under anaerobic conditions. NB: untreated bentonite as natural bentonite; BB: bacterial consortium; U: 1.26 mM uranyl acetate; e^-: 30 mM sodium acetate and 10 mM glycerol-2-phosphate as electron donors.

they may be interesting with regard to uranium tolerance. For microscopic observation, the isolates were Gram stained and examined in a LetizDialux 22 optic microscope. Genomic DNA was extracted from each colony by suspending a single pure colony in MilliQ water and heating for 10 min at 100 °C. The 16S rRNA gene of the extracted DNA was amplified using the universal bacterial primers 1492R (5'-TACGGYTACCTTGTTACGACTT-3') and 27F (5'-AAGAGTTTGATYMTGGCTCAG-3') and sequenced by bidirectional Sanger technology. The PCRs were performed using M.B.L. Recombinant Taq Polymerase kit (Material Blanco de Laboratorio, S.L., Spain) according to the manufacturer's instructions. PCR products were purified prior to sequencing using the Clean-Easy™ PCR Purification Kit (Canvax Biotech, Spain). The sequences were compiled and aligned using BioEdit. A comparative analysis was performed by matching these sequences with the ones in the GenBank database through the Basic Local Alignment Search Tool (BLAST).

2.3.2. Survival of SRB in Postgate medium

The viability of SRB was also studied in the U amended sample (T3_BBU). For this purpose, 1 g of bentonite slurry was added to 10 mL of Postgate medium (DSMZ_Medium63, https://www.dsmz.de) under anaerobic conditions to promote the growth of this group of bacteria. Postgate cultures were incubated for 4 weeks at 28 °C in the dark. The presence of black precipitates after the incubation time would indicate the growth of bacteria involved in sulfate reduction. DNeasy PowerSoil Pro Kit (Qiagen, https://www.qiagen.com/us) was used to extract total DNA from the Postgate cultures. DNA concentration measurements were performed as mentioned before.

The amplification, sequencing and analysis of the extracted DNA were carried out as previously mentioned for the total community (sections: 2.2.2 and 2.2.3).

2.4. Microscopic and spectroscopic characterization of the uranium-treated microcosm

High-resolution transmission electron microscope with high-angle annular dark-field (HAADF) imaging (Thermo Fisher Scientific TALOS F200X and FEI TITAN G2) coupled to energy dispersive X-ray spectroscopy (EDX) microanalysis was used to identify and characterize uranium accumulates after 3 months and 3 years of incubation. The acceleration voltage used to carry out the analysis was 200 kV. The intermediate layer formed between bentonite and supernatant was collected and prepared following the procedure used in Povedano-Priego et al., [27]. Selected area electron diffraction (SAED) and HRTEM combined with Fast Fourier Transform (FFT) were used to determine the crystalline nature of uranium precipitates.

Subsequently, the amended bentonite before ageing and the 3-year BBU microcosm were analyzed by X-ray photoelectron spectroscopy (XPS) to search for evidence of uranium phosphates. The interface between the bentonite and the supernatant of the BBU microcosm was sampled, dried, and pulverized. XPS measurements of this interface powder were conducted by Kratos AXIS Supra Photoelectron Spectrometer with a double anode X-ray source (Mg/Al) (Power 450 W). The source was monochromated Al Kα (power 600 W). High-resolution measurements of U 4f, P 2p, C 1s, O 1s, N 1s, Fe 2p and S 2p were performed, and deconvolution of the U 4f signal was performed (70 % Gaussian / 30 % Lorentzian line shape) to investigate potential element speciation. The software CasaXPS 2.3.22 [37] was used for the correction of the peaks in XPS spectra.

X-ray diffraction (XRD) was used to characterize the U solid phases which could be precipitated as result of the microbial activity within bentonite microcosms amended with this heavy metal. Powder XRD patterns of non-incubatedand incubated U-treated bentonites were recorded using a Bruker D8 Advanced diffractometer with Cu-Kα radiation linked to a LINXEYE detector available at "Centro de Instrumentation Cientifica", University of Granada. The obtained diffractograms were analysed using the software High Score+ and PDF2 database.

3. Results

3.1. Microbial diversity analyses: richness and distribution of the bacterial communities

The total DNA was extracted and sequenced in triplicate for all the treatments, including natural raw bentonite (NB). Two replicates, namely T3_BB3 and T3_BBU2, were excluded from the analysis due to their remarkable differences to the other replicates. Up to 390,112 sequences of 16S rRNA gene were gathered in 538 OTUs. Values of Good's coverage (> 0.99 % in all cases) indicated that the sequencing depth was enough to totally cover all the bacterial community (Table 1). The obtained OTUs were allocated in 30 phyla and 406 genera belonging to bacteria and Archaea. Only Halobacterota (2.21 % of OTUs) and Thermoplasmatota (0.03 % of OTUs) represented the Archaea whilst the other 28 phyla were bacteria. The most abundant bacterial phyla consisted of Proteobacteria (40.23 %), Firmicutes (27.33 %), Actinobacteriota (15.09 %) and Chloroflexi (5.78 %). The richness index (Sobs), diversity indices (ShannonH, and SimpsonD), and Shannon's evenness showed higher values in NB. However, the same indexes were lower at T0_BB and T0_BBU, indicating lower diversity and uniformity. On the other hand, higher alpha diversity was observed after 3 years, which also indicated higher diversity and uniformity at this time. All these data are shown in Table 1.

3.2. Effect of incubation time and uranium on the bentonite microbial diversity

At phylum level, the relative abundances changed depending upon the incubation time (Fig. 2). At time 0, in both treatments T0_BB (62.16 %) and T0_BBU (62.64 %), Proteobacteria was the most abundant phylum, mainly represented by two of the four bacterial consortium strains, *Pseudomonas* and *Stenotrophomonas* (Fig. 3, Supplementary Table S2). In the NB sample, Proteobacteria was also present at a relative abundance of 24.79 %. The other two most abundant phyla, Firmicutes [T0_BB (23.90 %); T0_BBU (26.17 %)] and Actinobacteriota [T0_BB (13.81 %); T0_BBU (11.10 %)] also mainly corresponded to the genera of the consortium *Bacillus* and *Amycolatopsis,* respectively. After the 3-year incubation, the relative abundances of Firmicutes were higher in T3_BB (48.94 %), and T3_BBU (44.64 %) compared to time 0 samples [T0_BB (23.90 %), and T0_BBU (26.17 %)]. Many Firmicutes are spore-formers, which allow them to survive in extreme environments for prolonged periods of time. However, Actinobacteriota decreased during the incubation period as most of them are aerobic. The incubation period also revealed phyla of interest to DGR such as Desulfobacterota, which includes most of the bacteria involved in the reduction of sulfate to sulfide. In the NB sample, its relative abundance was only 0.24 %, and < 0.001 % at time 0. Its enrichment was probably enhanced by the anaerobic conditions resulting in higher values of relative abundances [T3_BB (4.78 %), T3_BBU (2.99 %)]. Similarly, the two exclusive phyla within the Archaea domain,

Table 1
Richness (Sobs), diversity (ShannonH and SimpsonD), and evenness (ShannonE) indices and Good's coverage values of the bacterial communities of the different treatments. NB: raw natural bentonite; BB: bentonite inoculated with bacterial consortium; U: uranyl acetate 1.26 mM; T0: time 0; T3: three years of incubation.

Sample	Sobs	ShannonH	ShannonE	SimpsonD	Good's coverage
NB	437.99	6.80	0.78	0.98	0.999
T0_BB	57.30	2.47	0.42	0.76	0.999
T0_BBU	48.50	2.65	0.47	0.76	0.999
T3_BB	112.00	4.65	0.68	0.92	1.000
T3_BBU	132.34	4.92	0.69	0.93	0.999

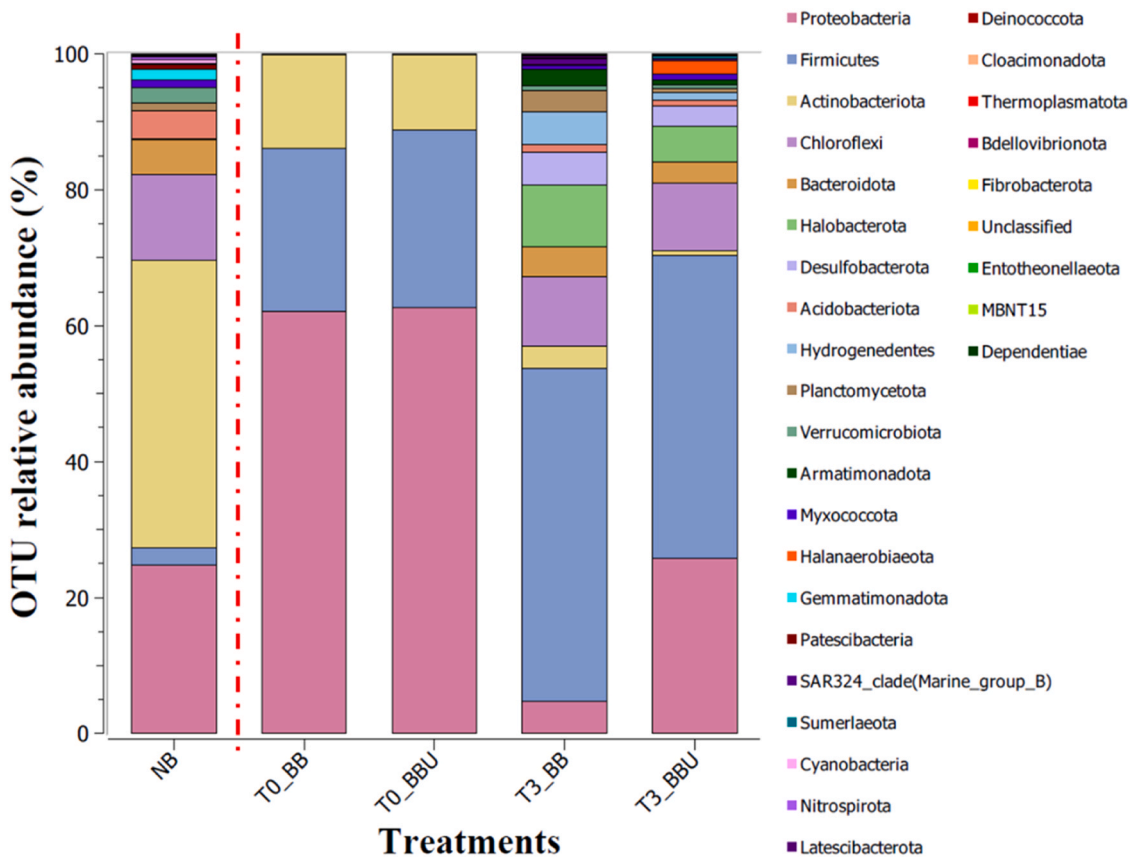

Fig. 2. Relative abundances of phyla belonging to Archaea and Bacteria in the raw natural bentonite and the treated water-saturated microcosms. Stacked bars represent the mean values of biological triplicates (except T3_BB and T3_BBU in duplicate). NB: raw natural bentonite; BB: bentonite inoculated with bacterial consortium; BBU: bentonite inoculated with bacterial consortium and treated with uranyl acetate; U: uranyl acetate 1.26 mM; T0: time 0; T3: three-year anoxic incubation.

Halobacterota (T3_BB (9.15 %), and T3_BBU (5.25 %)) and Thermoplasmatota (T3_BB (0.11 %), T3_BBU (0.07 %)) were slightly enriched in the 3-year incubated samples in comparison to T0 samples, where they were not detected.

The presence of uranium decreased the relative abundance of most phyla after the 3-year incubation, except for Firmicutes, Halanaerobiaeota, Sumerlaeota and Myxococcota, which increased to 20.93 %, 2.09 %, 0.32 %, and 0.29 %, respectively (Fig. 2, Supplementary Table S2).

At genus level (Fig. 3), in the natural bentonite, as expected, the four strains of the consortium (*Pseudomonas, Stenotrophomonas, Amycolatopsis,* and *Bacillus*) were detected at very low relative abundances (0.16 %, 0.01 %, 1.35 % and 1.15 %, respectively). At time 0, these genera displaced the remaining microbial diversity in both treatments, T0_BB and T0_BBU, dominating the total community with relative abundances of 89.42 % and 84.68 %, respectively.

The abundances of these genera decreased over time, and the overall community became more heterogeneous, as indicated by the previously mentioned alpha diversity data (Table 1) and the relative abundances after 3-year incubation (Supplementary Data S1). This decrease in dominance by the bacterial consortium, along with the incubation conditions, allowed the detection of other genera such as *Pelosinus* (T3_BB 22.91 %, T3_BBU 6 %), *Clostridium*_sensu_stricto_13 (T3_BB 7.91 %, T3_BBU 5.40 %), *Methanosacina* (T3_BB 7.36 %, T3_BBU 4.63 %), *Fonticella* (T3_BB 2.61 %, T3_BBU 5.73 %), unclassified Anaerolineaceae (T3_BB 5.31 %, T3_BBU 5.37 %), Peptostreptococcaceae (T3_BB 3.62 %, T3_BBU 5.04 %), *Anaerolinea* (T3_BB 4.43 %, T3_BBU 4.28 %), and *Lentimicrobium* (T3_BB 3.66 %, T3_BBU 2.92 %), among others. Concerning the bacteria involved in sulfate reduction (SRB), genera such as *Desulfovibrio* (T3_BB 2.95 %, T3_BBU 0.97 %), *Desulfosporosinus* (T3_BB 0.81 %, T3_BBU 1.55 %) and *Desulfobulbus* (T3_BBU 1.65 %) were also detected. Furthermore, apart from the previously mentioned *Methanosarcina*, other sequences affiliated with archaeal genera such as *Methanoculleus*, *Methanocella* and *Methanomassiliicoccus* were detected in low percentages of abundance (< 0.08 %) (Supplementary Data S1).

The influence of U toxicity on the microbial community within the bentonite slurry microcosms was remarkable. The relative abundance of certain genera decreased in the presence of uranium. This was the case, mainly, for *Pelosinus* (Δ −16.91 %), Hydrogenedensaceae (Δ −3.62 %), the archaea *Methanosarcina* (Δ −3.06 %), *Amycolatopsis* (Δ −2.57 %), and the sulfate-reducing bacterium *Desulfovibrio* (Δ −1.98 %). However, it is worth noting that another part of the community was enriched in the presence of this radionuclide. For instance, *Pseudomonas* (Δ 16.83 %), *Fonticella* (Δ 3.12 %), uncultured Lachnospirales (Δ 3.05 %), *Stenotrophomonas* (Δ 2.03 %), Peptostreptococcaceae (Δ 1.42 %) and *Sporacetigenium* (Δ 0.91 %) increased their relative abundance in the T3_BBU treatment. The SRB *Desulfobulbus* (Δ 1.65 %) and *Desulfosporosinus* (Δ 0.74 %) also increased in the presence of U.

The differences between the treatments have also been studied by the principal coordinate analysis (PCoA), considering only the BB and BBU samples. Based on the Bray-Curtis distance, PCoA analysis of relative abundance at genus level grouped the microcosms into three different clusters (Fig. 4). All the samples corresponding to time 0 (T0_BB and T0_BBU) were clustered into a single group and there were no differences between U-treated and control samples. However, after a three-year anaerobic incubation, the uranium treatment was separated from the controls. These results agreed with those obtained by the heatmap

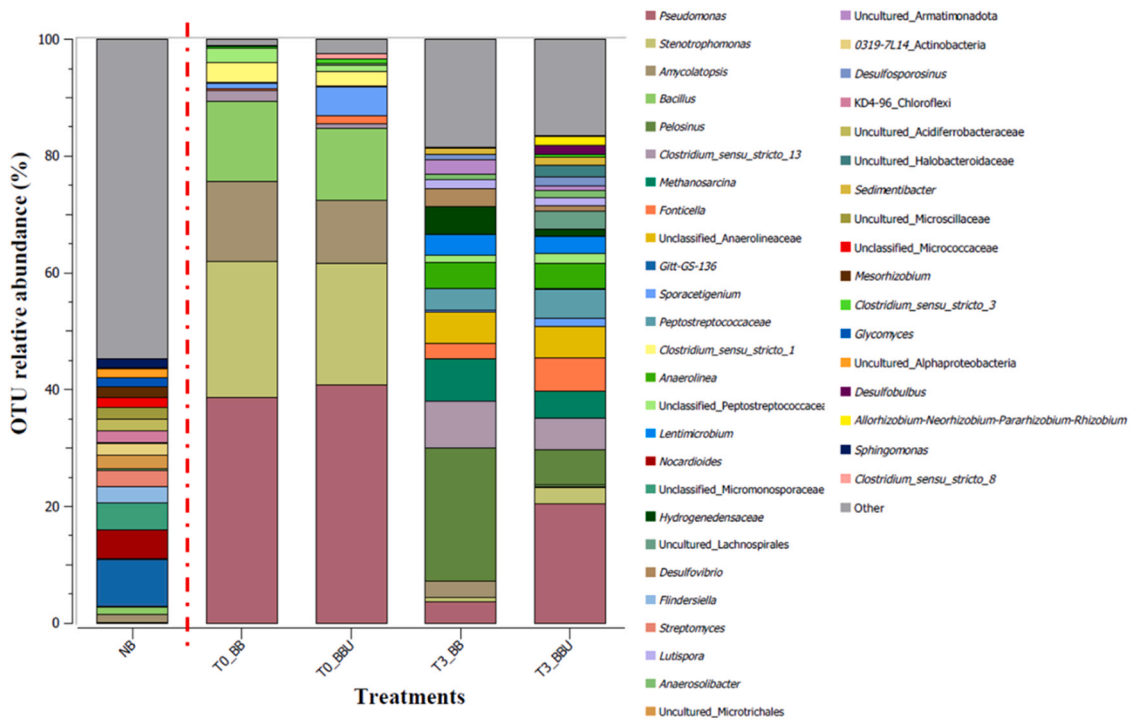

Fig. 3. Relative abundances at genus level of the microbial communities in raw natural bentonite and the water-saturated microcosms. Cut off: 0.3 % of relative abundance. Stacked bars represent the mean values of biological triplicates (except T3_BB and T3_BBU in duplicate). NB: raw natural bentonite; BB: bentonite inoculated with bacterial consortium; BBU: bentonite inoculated with bacterial consortium and treated with uranyl acetate; U: uranyl acetate 1.26 mM; T0: time 0; T3: three-year anoxic incubation.

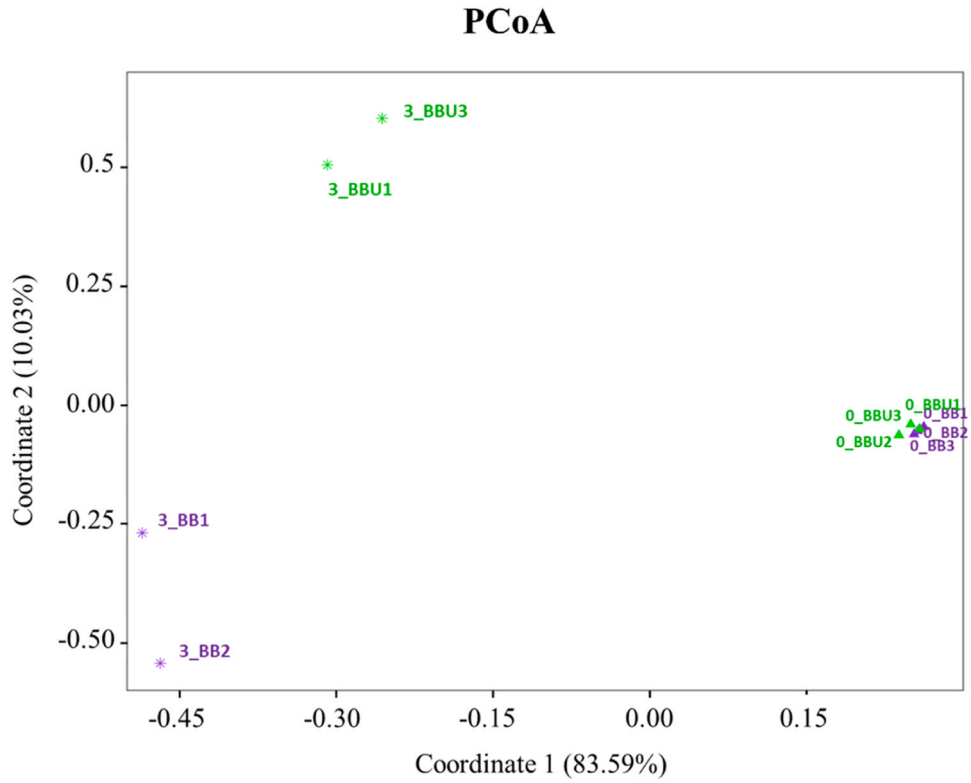

Fig. 4. Principal coordinate analysis (PCoA) comparing the microbial community structure of the different microcosms in triplicate (except T3_BB and T3_BBU in duplicate). The distance is based on Bray-Curtis algorithm. Triangle (▲): Time 0; Star (*): Time 3 years; purple color: controls without metal; green color: U-treatments. Samples studied in triplicates except T3_BB and T3_BBU in duplicate. BB: bentonite inoculated with bacterial consortium; BBU: bentonite inoculated with bacterial consortium and uranyl acetate; U: uranyl acetate 1.26 mM; T0: time 0: T3:3 -year incubation.

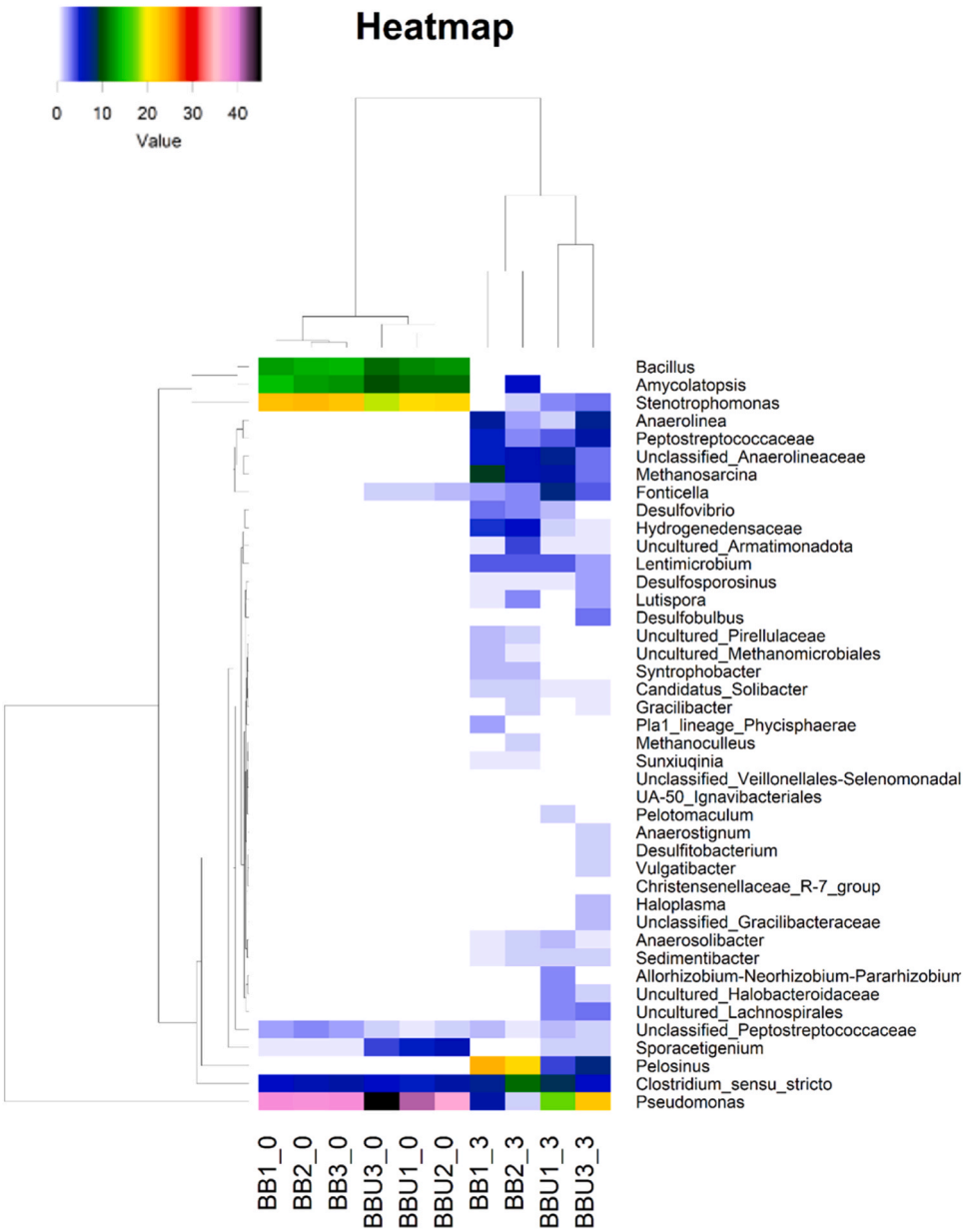

Fig. 5. Heatmap of relative abundances and microbial distribution of the samples based on Manhattan distance. Cut off: 1 %. Colors represent the varying levels of relative abundance for each genus. Samples studied in triplicates except T3_BB and T3_BBU in duplicate. BB: bentonite inoculated with bacterial consortium; BBU: bentonite inoculated with bacterial consortium and uranyl acetate; U: uranyl acetate 1.26 mM; T0: time 0; 3: 3-year incubation.

(Fig. 5), establishing a clear difference between the bacterial diversity of Time 0 samples and Time 3 years, as well as between 3-year samples with and without uranium.

3.3. Survival of bacterial strains after 3-year incubation

In this study, the long-term survival of aerobic heterotrophs was investigated by determining colony forming units (CFU) in 10 % LB culture medium, which was used to promote an oligotrophic environment. After 72 h of aerobic incubation, growth was observed in both treatments (T3_BB, T3_BBU). The viable heterotrophs counted in T3_BB were $(3 \pm 0.56) \times 10^4$ CFU/g, lower than that of the U amended sample ($(2.37 \pm 0.64) \times 10^5$ CFU/g).

The U-amended bentonite was selected to isolate strains that initially would have tolerated the presence of the radionuclide. A total of 5 strains were isolated from the 3-year U-amended bentonite sample (Table 2). Three out of 5 strains belonged to the genus *Peribacillus* (*P. frigoritolerans* WS2–1 16 S, *P. frigoritolerans* LZRD gt2, and *Peribacillus* sp. Sed8c), another to *Bacillus* (*B. korlensis* IHBB 9908), and the last one to *Robertmurraya* (*Robertmurraya* sp. TRM82488).

Table 2
Affiliation of the 16S rRNA of T3_BBU microbial isolates. BLAST revealed the closest phylogenetic relative strain, along with its similarity percentage and accession number.

Phylum	Isolate	Closest phylogenetic relative	Accession no., similarity (%)
Bacillota	BBU_1	*Peribacillus frigoritolerans* WS2-1 16S	MT605504.1, 98.39
Bacillota	BBU_2	*Peribacillus* sp. Sed8c	OR512255.1, 99.87
Bacillota	BBU_3	*Peribacillus frigoritolerans* LZRD gt2	OR079438.1, 100
Firmicutes	BBU_4	*Bacillus korlensis* IHBB 9908	KR085887.1, 99.42
Firmicutes	BBU_5	*Robertmurraya* sp. TRM82488	OR434954.1, 100

As mentioned above, the study of the sulfate-reducing bacteria is of great interest for the DGR safety assessment as they could be involved in the corrosion of the metal canisters where nuclear waste will be stored. SRB were enriched by the inoculation of U-amended bentonite sample (T3_BBU) in the Postgate medium. After 30 days of anaerobic incubation at 28 °C, a black precipitate was observed, which probably indicated the reduction of sulfate by SRB and formation of sulfides. Total DNA from this enrichment was extracted and the results showed that not only SRB were enriched (Fig. 6; Supplementary Data S2) since a total of 116 OTUs were detected in this sample. Genera such as *Sporacetigenium*, *Clostridium*, *Fonticella*, unclassified_Peptostreptococcaceae, *Pelosinus* and *Sedimentibacter* were the most abundant in agreement with the results of microbial diversity studies detailed above. Most of the identified strains are strict anaerobes, spore formers and capable of consuming some components present in the Postgate medium such as phosphate or lactate [38-41]. On the other hand, considering only the genera belonging to the SRB group, *Desulfovibrio,* and *Desulfosporosinus* were the most abundant with a relative abundance of 4.29 % and 1.97 %, respectively. Other genera such as *Desulfotomaculum*, *Syntrophomonas,* and *Desulfurispora* were also detected in low relative abundances (< 0.33 %). All these SRB would be responsible for using the sulfate in the medium and precipitating visible black sulfides (Fig. 6 C).

3.4. Microscopic (STEM-HAADF) cellular localization of the uranium accumulates over incubation time

After 3 months and 3 years of incubation, high-resolution transmission electron microscopy, coupled with energy dispersive X-ray spectroscopy (EDX), was used to study the cellular location of U accumulates and their chemical properties in the BBU sample. At both incubation times, the bentonite of the microcosm corresponding to the BBU treatment presented a grayish color compared to time 0 (Supplementary Fig. S1). The intermediate layer formed between bentonite and supernatant was collected and microscopically analyzed.

After 3 months of incubation, STEM-HAADF micrographs showed electron-dense accumulates at the cell wall level (Fig. 7 A). The EDX spectra and maps analyses revealed U and P as elemental composition of U accumulates (Fig. 7 B, C, E). Selected area electron diffraction (SAED) and HRTEM combined with Fast Fourier Transform (FFT) were used to determine the crystalline nature of these precipitates. These parameters showed no signal, which implies an amorphous nature (Fig. 7 D). Moreover, the cytoplasm of certain cells exhibited the presence of U signal (Fig. 7 G, J, L). The identified uranium also aligned with the P signal as shown in Fig. 7 H, K, L.

On the other hand, after 3 years of anoxic incubation, the U signal was not found in the extracellular space either. It was noteworthy that the abundance of bacterial cells was minimal, and the predominant ones displayed a morphology characteristic of bacterial spores (Supplementary Fig. S2). Additionally, most of the cells exhibited damaged cell walls (Fig. 8).

At 3-year incubation time, U was only localized in the inner part of the cell wall area (Fig. 8 A, B). The EDX analyses confirmed the presence of both U and P signals, which is consistent with the observations made on the 3-month sample but with Ca also present (Fig. 8 C, E, F). These electron-dense zones were analyzed with SAED and FFT indicating amorphous nature of the accumulates. (Fig. 8 D).

3.5. X-ray photoelectron spectroscopy and X-ray diffraction: Characterization of uranium species in U-bentonite microcosm

XPS analysis was undertaken to assess the presence of U in the samples before and after the 3-year incubation time. XPS peaks corresponding to U 4f were weak and with a high signal-to-noise ratio given the low concentration expected in the bentonite samples; however, their presence was still evident. A peak around 378.5 eV was attributed to the presence of potassium from the natural bentonite (K 2s), which makes the deconvolution and analysis of U 4f peaks more difficult. At T_0, the high resolution XPS spectra showed a U $4f_{7/2}$ peak at 385.4 eV, which has previously been assigned as U(VI) sorbed on montmorillonite [42]. After the 3-year incubation, an additional peak was observed at 381.6 eV, which has previously been reported as $U(UO_2)\cdot(PO_4)_2$ [43]. The peak assigned to $U(UO_2)\cdot(PO_4)_2$ in the aged sample (T3_BBU treatment) was absent in the T_0 (see Fig. 9). XPS signals usually attributed to U(IV) species as uraninite have been previously reported at 378.1 eV [44]. However, in the high-resolution scans shown in Fig. 9, this signal also coincides with the peak of K 2s. Therefore, the confirmation of uraninite via XPS is less reliable. In order to validate the above observations, and given the difficulty of analyzing the U 4f peak due to its weak intensity and interference with the K 2s signal, the samples were also examined using X-ray diffractometry.

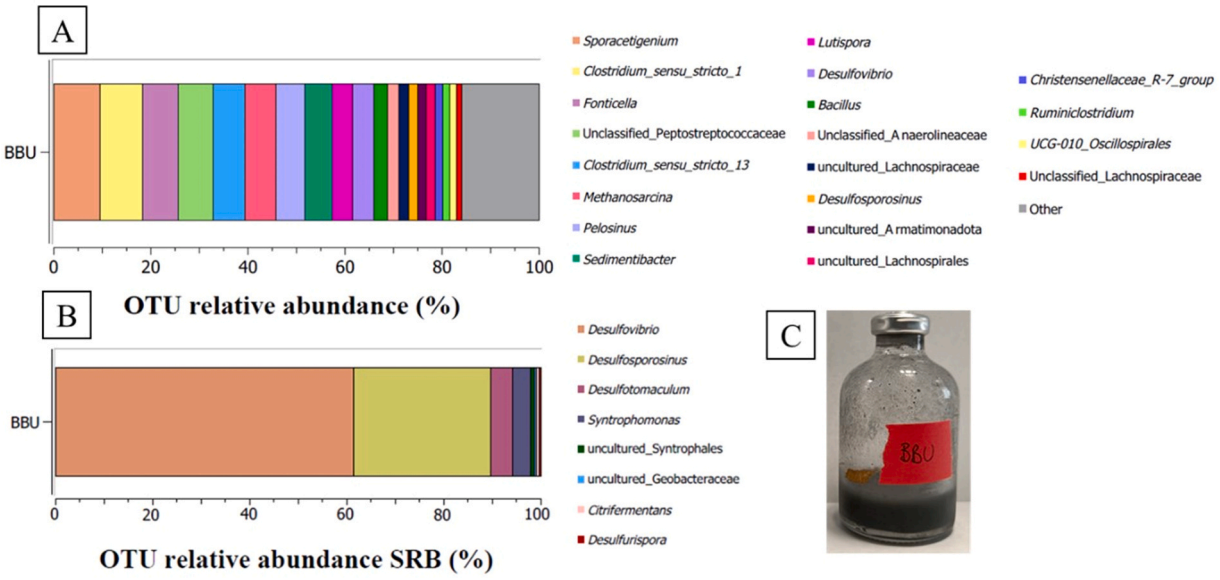

Fig. 6. A. OTU relative abundances at genus level of the T3_BBU microbial communities enriched in Postgate medium. Cut off: 1 % of relative abundance. Stacked bars represent the mean values of biological triplicates. B. OTU relative abundances at genus level of the main SRB communities enriched in Postgate medium. C. Postgate medium inoculated with T3_BBU bentonite after 30-day anaerobic incubation at 28 °C.

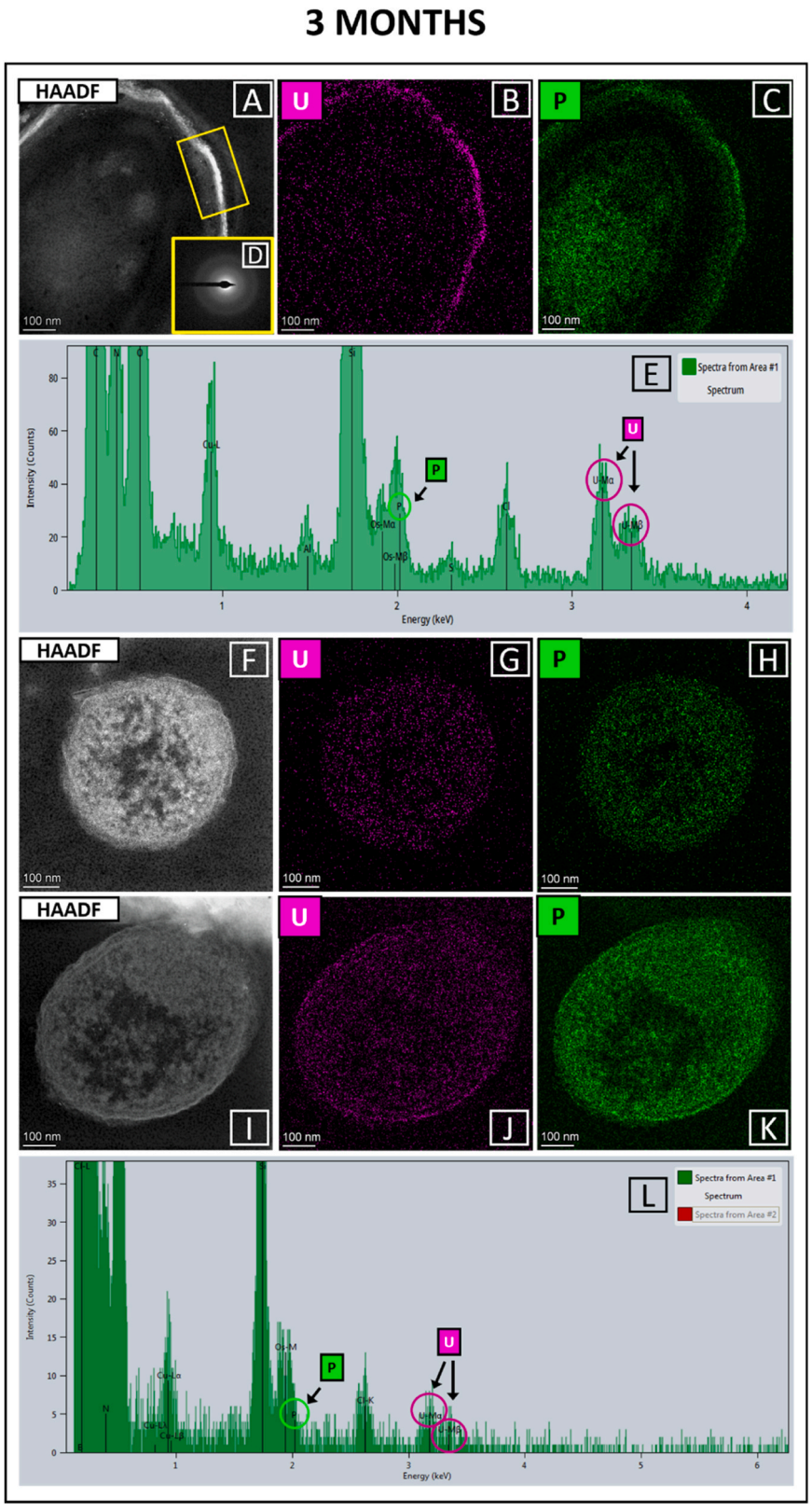

Fig. 7. Scanning transmission electron microscopy-high-angle annular dark-field imaging (STEM-HAADF) image of BBU microcosm after 3-month incubation (A, F, I). The EDX maps with the elemental distribution of U in pink color, and P in green color (B, C, G, H, J, K) and their corresponding EDX spectra (E, L). The SAED pattern of selected area in A corresponds to the amorphous form of U-phosphates (D).

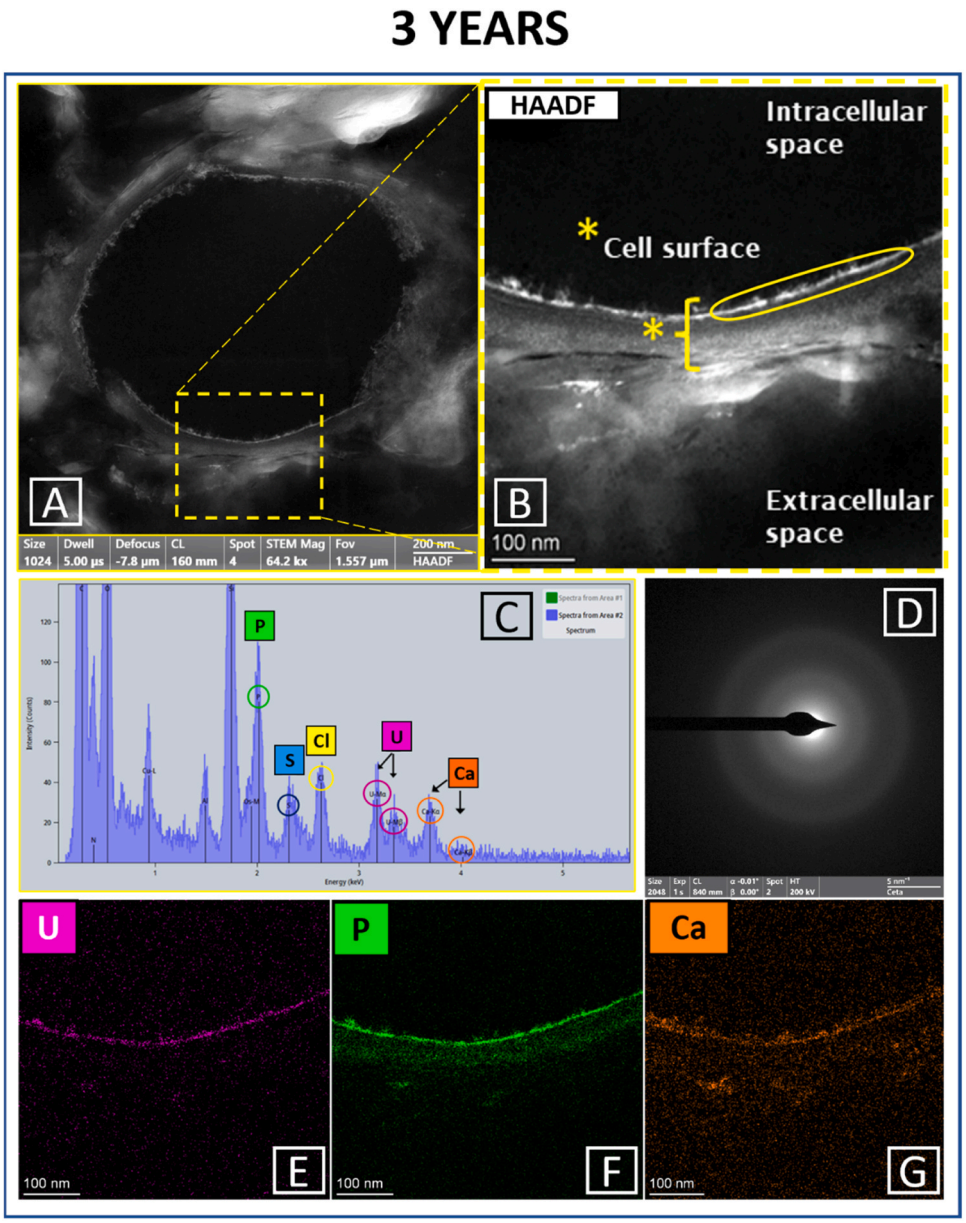

Fig. 8. Scanning transmission microscopy-high-angle annular dark-field imaging (STEM-HAADF) image of BBU microcosm after 3-year incubation (A). Expanded image of A (B). The EDX maps with the elemental distribution of U in pink color, P in green color and Ca in orange color (E, F, G) and the corresponding EDX spectrum (C). The SAED pattern of selected area in B corresponds to the amorphous form of U-phosphates (D).

The XRD pattern of the non-incubated bentonite was similar to that of natural Spanish bentonite reported by Povedano-Priego et al., [25]. The bentonite consisted of at least 91 % of smectite and accessory minerals in minor amounts (quartz, plagioclases, micas, cristobalite). No U mineral phases were detected.

The XRD patterns obtained for the 3-year U-treated bentonite microcosms showed the main peaks characteristic of Spanish bentonite corresponding to major mineral phases like smectite and to minor phases (e.g. quartz), and calcite as well. In addition, the XRD diffractogram (Supplementary Fig. S3) showed also the presence of a peak at 9.88 °2θ, and small peaks at 10.2–9.60 °2θ, corresponding to uranium phosphate minerals of the autunite or meta-autunite group, including autunite (Ca), sodium autunite (Na) and saleeite (Mg). Other two small peaks at 27.73 (as a shoulder on the plagioclase peak at 27.90) and 31.13 °2θ might correspond to uraninite (UO_2).

3.6. pH analysis of microcosm supernatants over incubation time

At time 0, 3, 6 and 9 months, and 3 years, supernatant samples were collected from the three replicates of each treatment (BB and BBU) to measure the pH. At the beginning of incubation, both microcosms had neutral pH values (around 7.4). During the first months of incubation (3, 6 and 9), the pH of both treatments increased until reaching basic values of 8.72 for BB and 8.86 for BBU (Supplementary Table S3). The pH evolution over time was similar in both cases, indicating that there were no notable differences between the treatment values. After the 3-year incubation, the pH value for each treatment was around 8.

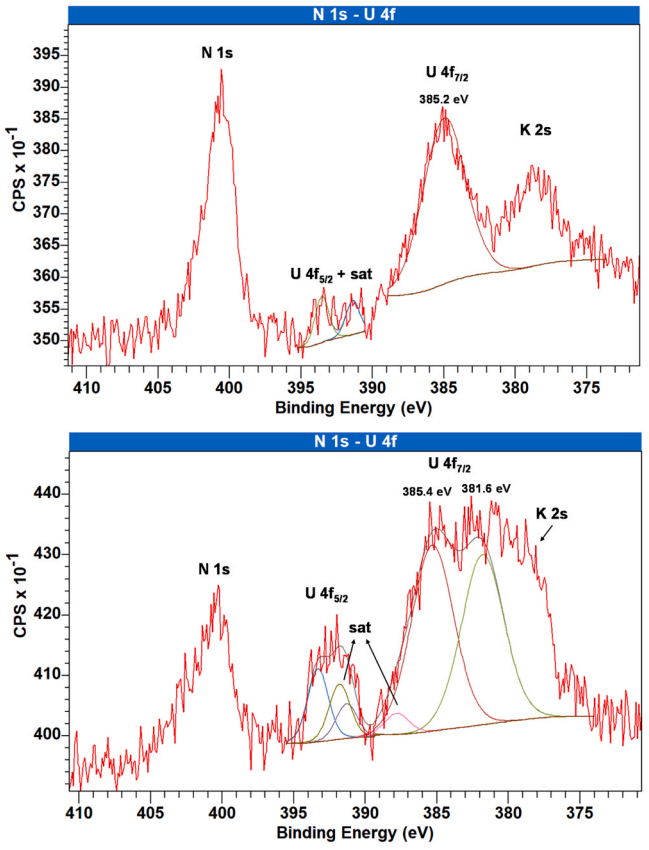

Fig. 9. High resolution X-ray photoelectron spectra of the U(4 f) region for samples before (top) and after the 3-year incubation time (bottom).

4. Discussion

4.1. Influence of incubation time and uranium on bentonite microbial diversity

To accelerate the microbial processes that would occur in the bentonite barrier, the microcosms were amended with electron donors and inoculated with a bacterial consortium (BB) which is composed of 4 genera previously identified in bentonite [11,13,16,25]. In addition, the experimental conditions of this study would simulate the scenario of filtration of groundwater loaded with organic compounds within the bentonite body during the disposal period [45].

Throughout the incubation time many changes were observed to occur between the time 0 (T0_BB, T0_BBU) and the 3-year (T3_BB, T3_BBU) microcosms. The bacterial diversity increased considerably after 3 years of incubation, compared to time 0 where the four strains of the consortium almost completely dominated the community. The long-term incubation of the samples allowed the community to shift completely, leading to the enrichment of anaerobic and spore-forming bacteria. The microbial communities were dominated by representatives of the phylum Firmicutes, which includes most genera capable of forming endospores in adverse conditions [46]. HRTEM microscopy images corroborated the presence of bacterial spores, as shown in Supplementary Fig. S2. Another phylum that stood out was Chloroflexi that includes most anaerobic genera (e.g. *Anaerolinea*) [47], whilst the phylum Actinobacteriota, dominant in both NB and at time 0 microcosms (T0_BB, T0_BBU), decreased drastically, probably because the majority of bacteria belonging to this phylum are aerobic [48]. The experimental anoxic conditions also favored the presence of anaerobic genera, such as the archaea *Methanosarcina* and the sulfate-reducing group of bacteria such as *Desulfovibrio*, *Desulfosporosinus* and *Desulfobulbus*. These findings align with the expected scenario in future DGRs, where upon the repository closure, oxic conditions will initially be contemplated. As time progresses a transition towards reducing conditions is foreseen, marked by the prevalence of anaerobic bacterial communities [4]. The comparison of the microbial population incubated for 3 years showed that the presence of uranium seemed to differentially affect the relative abundance of some taxon in the bentonite. However, the most affected genera are playing a key role in the biogeochemical cycle of this radionuclide through different processes such as U phosphate biomineralization, enzymatic U(VI) reduction to uraninite (U(IV) O_2), and biosorption, amongst others [6,25,49,50]. These results could be supported by a combination of XPS, XRD, STEM and EDX data, indicating that the U speciation is likely to be governed by U(VI) and U (IV) as phosphate mineral phases of the autunite or meta-autunite groups and uraninite, respectively.

In our study, some strains of notable importance in interactions with uranium, such as *Pseudomonas* and *Stenotrophomonas*, were enriched in the treatment with this radionuclide (T3_BBU). Several studies have demonstrated the ability of *Pseudomonas* to immobilize U through different processes including biosorption, biomineralization, and bioreduction [51,52]. Therefore, its presence and predominance under these conditions was not unexpected, since it is demonstrated to be a naturally occurring bacterium in uranium mines and it was also detected in uranium-treated bentonites incubated for six months under anoxic conditions [26,53,54]. Regarding *Stenotrophomonas*, this bacterium has also been previously studied for its ability to interact and resist U(VI) [50,55,56]. Like *Pseudomonas*, this genus, specifically the species *S. bentonitica,* is one of the strains of the consortium added to the bentonite microcosms as it was previously isolated and characterized from Spanish bentonite samples [57]. Two additional genera, namely *Fonticella* and *Sporacetigenium*, exhibited an increase in their relative abundance in the U-treatment. So far, no information exists explicitly linking these two strains to metal resistance, but the ability to withstand harsh environments may explain their presence under such DGR relevant conditions [58–61].

On the other hand, the presence of uranium seemed to decrease the relative abundance of other microbes including *Pelosinus*, *Hydrogenedensaceae*, *Methanosarcina*, *Amycolatopsis* and *Desulfovibrio* that have the capacity to immobilize uranium [25,62-64]. However, despite of this decrease in relative abundance, the presence of these genera in the U amended samples would affect the U biogeochemistry. For instance, even if the relative abundance of *Desulfovibrio* and *Methanosarcina* was decreased, they may still exhibit the ability to reduce U(VI) to U(IV), as reported by Sani et al., [64] and Holmes et al., [62], respectively. In our study, *Desulfovibrio* was dominating the enriched SRB population in the Postgate medium and *Methanosarcina* also appeared as viable archaea in this medium after 3 years in T3_BBU. In addition, Thorgersen et al. [65], demonstrated that surface layer proteins of *Pelosinus*, also viable in Postgate enrichment, were able to bind U through carboxyl and phosphate groups resulting in biosorption processes.

The presence of viable bacteria after 3 years of incubation was demonstrated in the present study. *Peribacillus*, *Bacillus* and *Robertmurraya* were isolated and identified in the T3_BBU treatment. This was in accordance with Babich et al. [66], who reported having isolated a strain aligning with the genus *Peribacillus* from sub-surface horizons of a uranium deposit in Russia. Kumari et al. [67] also isolated *Bacillus korlensis* from acidic copper mines, which implies its resistance in extreme environments. The last isolate was identified as *Robertmurraya* sp. This genus previously corresponded to *Bacillus,* and was reclassified in 2020 [68,69]. Therefore, there is no information on the relationship of this genus with uranium but the resistance of the *Bacillus* genus to this metal is very well documented [70-72].

As mentioned above, the enrichment in the Postgate medium of the uranium-treated bentonite (BBU) revealed the presence of viable SRB after 3 years of incubation. Several SRB are described for their capability to reduce U, being detected even in uranium mines [64,73,74].

Reportedly, some SRB possess outstanding U(VI) reduction capacity through processes involving c-type cytochromes, extracellular pili, electron shuttle, or thioredoxin reduction [24]. The key role of these bacteria in the reduction of U(VI) to U(IV) could be supported by XRD data and the detection of uranium signal in the cell wall and inside the cytoplasm of different bacterial cells by STEM and EDX microscopy (see Figs. 7, 8).

4.2. Chemical speciation of U throughout the incubation time: influence of bentonite microbial community

The impact of microbial communities of the 3-year U amended bentonites in the chemical speciation of U was characterized by a combination of microscopic (STEM/HAADF/EDX) and spectroscopic (XPS and XRD) techniques. Both complementary methods showed the key role of biotic processes in affecting the U complexation. However, abiotic processes mediated by clay minerals can also be one of the main contributors to the fate of U in the studied samples. For example, Lee & Lee [75] and Wazne et al., [76] reported the adsorption capacity of minerals such as pyrite and other adsorbents (e.g. aluminum oxides and ferric oxyhydroxides) to uranium cations. Additionally, abiotic uranium reduction processes may have occurred. This involves the indirect reduction of U(VI) through Fe(II) produced by microbes utilizing Fe (III)-containing clays and oxides as terminal electron acceptors for anaerobic respiration [77,78]. Tsarev et al., [79] reported that such electron transport systems can also be established by adsorbing Fe(II) ions on mineral surfaces, and reduced U(IV) species can subsequently be adsorbed on mineral surfaces or transformed into nanocrystalline uraninite, depending on pH values. Humic acids are also acknowledged to play a role in redox reactions, including the abiotic reduction of U(VI) [78]. In addition, the hydrogen sulfide, resulting from sulfate reduction by SRB, can abiotically reduce U(VI) to U(IV) or react with iron to form ferrous sulfide precipitates that may also reduce U(VI) [80]. The XPS data suggested two different U species which would correspond to U(VI) phosphate mineralization as $U(UO_2)\cdot(PO_4)_2$ and U(VI) adsorption to clay minerals from the montmorillonite group. In addition, the XRD patterns obtained for the 3-year U-treated bentonite microcosms detected the presence of uranium phosphate minerals of the autunite or meta-autunite group and suggested the presence of uraninite. The formation of biogenic U(VI) phosphates was confirmed by electron microscopy and supported by microbial diversity data. STEM/HAADF/EDX analysis showed the presence of amorphous U phosphate accumulates in the inner part of the bacterial cell membranes indicating the key role of biotic processes in the U speciation in the studied ternary system. These U phosphates accumulates could correspond to meta-autunite mineral group, which was well described to be one the most U phosphate precipitated by bacteria [81]. It is well known that autunite phases are normally characterized by tetragonal morphology, including autunite and meta-autunite minerals such as chernikovite, meta-ankoleite, and sodium meta-autunite. It is possible that due to the high sensitivity of water retention to temperature, the loss of water during HRTEM could influence the interlayer configuration and hydrogen bonding, potentially causing a collapse in the crystal structure [82]. Hufton et al. [83] have reported the ability of U(VI) to interact with the different components of the cell wall and cell membrane such as phospholipids and associated proteins of both gram-negative and gram-positive bacteria. They discussed that uranium ions could pass through the pores of the peptidoglycan due to their small size, facilitating the sorption process to the most inner compounds of the cell membrane and consequent U complexation. U phosphate biomineralizing bacteria such as *Pseudomonas* and *Stenotrophomonas* were enriched in the U amended sample. Sanchez-Castro et al., [56] have reported the biomineralization of U(VI) phosphates in the cell membrane of *Stenotrophomonas* sp. leading to the removal of about 98 % of U from solution. This process was mediated by phosphatase activity located in the cell membrane, which cleaves organic phosphate substrate (G6P) releasing orthophosphates for the precipitation of this radionuclide. The U phosphate biomineralization by *Pseudomonas* has also been well documented [54]. Additionally, two small peaks likely corresponding to uraninite (UO_2) were observed by XRD. Thus, SRB from the genera *Desulfovibrio*, *Desulfosporosinus*, *Desulfotomaculum*, that prevail microbial diversity, were reported to reduce U(VI) to U(IV) [64, 73,74]. No uraninite was detected by electron microscopy. Alessi et al. [84] reported that uraninite usually lacks a crystalline structure, being less stable and easily re-oxidizable. In the same study, they demonstrated the ability of non-crystalline U(IV), coming from the reduction of U(VI) on the cell wall, to bind to free phosphate groups resulting in the formation of U(IV)-phosphate nanoparticles. This substantiates the hypotheses regarding uranium interactions, as evidenced by the detected peaks corresponding to uraninite (UO_2), indicative of a likely bioreduction process [44]. The U(VI) binding by montmorillonite through a sorption process has also been reported [42,43]. Uraninite deposits have been previously reported in several studies in the cytoplasmic space of genera like *Pseudomonas* and *Desulfovibrio* [85,86]. Merroun and Selenska-Pobell [21] hypothesized the potential diffusion of reduced uranium nanoparticles from the periplasm to the cytoplasm. However, the potential processes leading to intracellular uraninite precipitation remain unresolved.

Likewise, it is important to consider a potential abiotic reduction of U (VI). For example, the reduction by the hydrogen sulfide or Fe(II) resulting from sulfate reduction by SRB and Fe(III) reduction by IRB, respectively, in addition to the possible involvement of humic acids [77-80]. Therefore, in the present study, U(VI) could be reduced not only directly by bacterial activity but also through various abiotic redox reactions.

The results presented and discussed in this work constitute a preliminary investigation into the potential effects of detrimental conditions, such as uranium leakage, groundwater infiltration, and bacterial activity on a heterogeneous and complex system like a future nuclear repository. Based on these initial findings, further studies could be conducted to elucidate at atomic and molecular scale the local coordination of U in the bentonite microcosms, obtaining more detailed understanding of the different biogeochemical processes that may occur. This could be achieved using spectroscopic techniques based on synchrotron radiation like EXAFS/XANES, micro-EXAFS, and X-ray microscopy.

5. Conclusions

Here, we provide clear experimental evidence that uranium and long-term incubation can shift microbial populations in bentonite microcosms amended with nutrients within the context of DGR. The 3-year incubation period entirely shaped the microbial diversity, favoring the prevalence of anaerobic and spore-forming microorganisms mainly from the phylum Firmicutes and Chloroflexi in addition to SRB. Viable SRB like *Desulfovibrio* and *Desulfosporosinus* were enriched from U amended bentonite microcosms indicating their tolerance to this radionuclide. U amendment increased the relative abundance of microbial strains involved in the U biogeochemical cycling of U through U phosphate biomineralization (e.g. *Pseudomonas* and *Stenotrophomonas*) and U reduction as uraninite (e.g. *Desulfovibrio*). We demonstrated that the uranium speciation was significantly affected by the bentonite microbial populations in 3 years. A combination of XPS, XRD and STEM/HAADF analyses showed that U was present as U(VI) and U(IV) species. In the case of U(VI), biogenic U(VI) phosphates located in the inner part of the bacterial cell membranes in addition to U(VI)-adsorbed to clays such as montmorillonite were detected. XRD identified U-phosphate as autunine or meta- autunite group. Biogenic U(IV) species such as uraninite may be produced as a result of bacterial enzymatic reduction of U(VI). These results showed that bentonite microbes might be able to interact with U (VI) through U phosphate biomineralization and U(VI) reduction to U (IV) and the formation of uraninite. Abiotic processes would also govern

the U fate through its sorption to bentonite clay or abiotic reduction. However, further research is required to elucidate which of the mentioned interaction processes would be conducted by viable bacteria to immobilize such toxic radionuclide in DGR relevant conditions. Nevertheless, these findings offer novel insights into the long-term behavior of bentonite micro organisms in the event of a potential release of one of the most critical waste elements in conjunction with simulated groundwater seepage.

Environmental implications

Ensuring future nuclear waste repository safety requires consideration of physicochemical and microbiological factors. This study provides novel insights into microbial behavior in bentonite barriers, addressing worst-case scenarios like waste leakage (e.g., uranium) and groundwater infiltration. We present evidence of the enrichment of anaerobic and spore-forming microbes and viable sulfate-reducing bacteria (SRB) upon U-amended bentonite after a 3-year incubation. Furthermore, U speciation was affected by both biotic and abiotic processes, leading to its immobilization as U(VI) phosphates, uraninite, in addition to its sorption onto bentonite minerals. This implies that the U-immobilization within this barrier could positively enhance the safety performance of future DGRs

Funding

This study was supported by the grant RTI2018-101548-B-I00 “ERDF A way of making Europe” to MLM from the “Ministerio de Ciencia, Innovación y Universidades” (Spanish Government). The project leading to this application has received funding from the European Union’s Horizon 2020 research and innovation program under grant agreement No 847593 to MLM and the grant FPU20/00583 to the first author from the “Ministerio de Universidades” (Spanish Government).

CRediT authorship contribution statement

Mar Morales-Hidalgo: Writing – review & editing, Writing – original draft, Visualization, Validation, Methodology, Investigation, Formal analysis, Conceptualization. **Cristina Povedano-Priego:** Writing – review & editing, Visualization, Validation, Methodology, Investigation, Formal analysis. **Marcos F. Martinez-Moreno:** Writing – review & editing, Investigation. **Jesus J. Ojeda:** Writing – review & editing, Visualization, Formal analysis. **Fadwa Jroundi:** Writing – review & editing, Validation, Methodology, Investigation, Formal analysis. **Mohamed L. Merroun:** Writing – review & editing, Writing – original draft, Validation, Supervision, Resources, Project administration, Methodology, Funding acquisition, Formal analysis, Conceptualization.

Declaration of Competing Interest

The authors declare that they have no known competing financial interests or personal relationships that could have appeared to influence the work reported in this paper.

Data availability

The nucleotide sequences and metagenomics’ raw data of this study were submitted to the sequence read archive (SRA) at NCBI: BioProject accession number PRJNA1083466.

Acknowledgements

The authors acknowledge the assistance of Dr. F. Javier Huertas (IACT, Spain) for his guidance and help in collecting the bentonite from the deposit of Almería and Concepcion Hernandez-Castillo and Daniel García Muñoz Bautista Cerro for the preparation of samples for microscopic analyses. We also acknowledge the assistance of Dr. María del Mar Abad Ortega and other members of Centro de Instrumentación Científica (University of Granada, Spain) for the microscopy assistance. Funding for open access charge: Universidad de Granada / CBUA.

Appendix A. Supporting information

Supplementary data associated with this article can be found in the online version at doi:10.1016/j.jhazmat.2024.135044.

References

[1] Othman, S.A. (2023). Nuclear Energy From Current Perspective: A Short Review. Enhanced Knowledge in Sciences and Technology, 3(1), 011–015. Retrieved from https://penerbit.uthm.edu.my/periodicals/index.php/ekst/article/view/5578.
[2] Tondel, M., Lindahl, L., 2019. Intergenerational ethical issues and communication related to high-level nuclear waste repositories. Curr Environ Health Rep 6 (4), 338–343. https://doi.org/10.1007/s40572-019-00257-1.
[3] WNA. World Nuclear Association. (2021). Storage and disposal of radioactive waste. ⟨https://www.world-nuclear.org/⟩.
[4] Duro, L., Domènech, C., Grivé, M., Roman-Ross, G., Bruno, J., Källström, K., 2014. Assessment of the evolution of the redox conditions in a low and intermediate level nuclear waste repository (SFR1, Sweden). Appl Geochem 49, 192–205. https://doi.org/10.1016/j.apgeochem.2014.04.015.
[5] Hall, D.S., Behazin, M., Binns, W.J., Keech, P.G., 2021. An evaluation of corrosion processes affecting copper-coated nuclear waste containers in a deep geological repository. Prog Mater Sci 118, 100766. https://doi.org/10.1016/j.pmatsci.2020.100766.
[6] Ruiz-Fresneda, M.A., Martinez-Moreno, M.F., Povedano-Priego, C., Morales-Hidalgo, M., Jroundi, F., Merroun, M.L., 2023. Impact of microbial processes on the safety of deep geological repositories for radioactive waste. Front Microbiol 14, 1134078. https://doi.org/10.3389/fmicb.2023.1134078.
[7] Kuleshova, M.L., Danchenko, N.N., Sergeev, V.I., Shimko, T.G., Malashenko, Z.P., 2014. The properties of bentonites as a material for sorptive barriers. Mosc Univ Geol Bull 69, 356–364. https://doi.org/10.3103/S0145875214050044.
[8] Villar, M.V., Pérez del Villar, L., Martín, P.L., Pelayo, M., Fernández, A.M., Garralón, A., et al., 2006. The study of Spanish clays for their use as sealing materials in nuclear waste repositories: 20 years of progress. J Iber Geol 32, 15–36.
[10] Burzan, N., Murad Lima, R., Frutschi, M., Janowczyk, A., Reddy, B., Rance, A., et al., 2022. Growth and persistence of an aerobic microbial Community in Wyoming Bentonite MX-80 despite anoxic in situ conditions. Front Microbiol 13, 858324. https://doi.org/10.3389/fmicb.2022.858324.
[11] Lopez-Fernandez, M., Fernández-Sanfrancisco, O., Moreno-García, A., Martín-Sánchez, I., Sánchez-Castro, I., Merroun, M.L., 2014. Microbial communities in bentonite formations and their interactions with uranium. Appl Geochem 49, 77–86. https://doi.org/10.1016/j.apgeochem.2014.06.022.
[12] Lopez-Fernandez, M., Cherkouk, A., Vílchez-Vargas, R., Jauregui, R., Pieper, D., Boon, N., et al., 2015. Bacterial diversity in bentonites, engineered barrier for deep geological disposal of radioactive wastes. Microb Ecol 70, 922–935. https://doi.org/10.1007/s00248-015-0630-7.
[13] Lopez-Fernandez, M., Romero-González, M., Günther, A., Solari, P.L., Merroun, M. L., 2018. Effect of U(VI) aqueous speciation on the binding of uranium by the cell surface of *Rhodotorula mucilaginosa*, a natural yeast isolate from bentonites. Chemosphere 199, 351–360. https://doi.org/10.1016/j.chemosphere.2018.02.055.
[9] Bengtsson, A., Pedersen, K., 2017. Microbial sulphide-producing activity in water saturated Wyoming MX-80, Asha and Calcigel bentonites at wet densities from 1500 to 2000 kg·m^{-3}. Appl Clay Sci 137, 203–212. https://doi.org/10.1016/j.clay.2016.12.024.
[14] Martinez-Moreno, M.F., Povedano-Priego, C., Morales-Hidalgo, M., Mumford, A.D., Ojeda, J.J., Jroundi, F., et al., 2023. Impact of compacted bentonite microbial community on the clay mineralogy and copper canister corrosion: a multidisciplinary approach in view of a safe Deep Geological Repository of nuclear wastes. J Hazard Mater, 131940. https://doi.org/10.1016/j.jhazmat.2023.131940.
[15] Masurat, P., Eriksson, S., Pedersen, K., 2010. Evidence of indigenous sulphate-reducing bacteria in commercial Wyoming bentonite MX-80. Appl Clay Sci 47 (1-2), 51–57. https://doi.org/10.1016/j.clay.2008.07.002.
[16] Povedano-Priego, C., Jroundi, F., Lopez-Fernandez, M., Shrestha, R., Spanek, R., Martín-Sánchez, I., et al., 2021. Deciphering indigenous bacteria in compacted bentonite through a novel and efficient DNA extraction method: Insights into biogeochemical processes within the Deep Geological Disposal of nuclear waste concept. J Hazard Mater 408, 124600. https://doi.org/10.1016/j.jhazmat.2020.124600.
[17] Yang, S., Li, S., Jia, X., 2019. Production of medium chain length polyhydroxyalkanoate from acetate by engineered *Pseudomonas putida* KT2440. J Ind Microbiol Biotechnol 46 (6), 793–800. https://doi.org/10.1007/s10295-019-02159-5.
[18] Lopez-Fernandez, M., Jroundi, F., Ruiz-Fresneda, M.A., Merroun, M.L., 2021. Microbial interaction with and tolerance of radionuclides: underlying mechanisms and biotechnological applications. Microb Biotechnol 14 (3), 810–828. https://doi.org/10.1111/1751-7915.13718.

[19] Martínez-Rodríguez, P., Sánchez-Castro, I., Ojeda, J.J., Abad, M.M., Descostes, M., Merroun, M.L., 2023. Effect of different phosphate sources on uranium biomineralization by the *Microbacterium* sp. Be9 strain: a multidisciplinary approach study. Front Microbiol 13, 1092184. https://doi.org/10.3389/fmicb.2022.1092184.

[20] Merroun, M., Nedelkova, M., Rossberg, A., Hennig, C., Selenska-Pobell, S., 2006. Interaction mechanisms of bacterial strains isolated from extreme habitats with uranium. Radiochim Acta 94 (9-11), 723–729. https://doi.org/10.1524/ract.2006.94.9-11.723.

[21] Merroun, M.L., Selenska-Pobell, S., 2008. Bacterial interactions with uranium: an environmental perspective. J Contam Hydrol 102 (3-4), 285–295. https://doi.org/10.1016/j.jconhyd.2008.09.019.

[22] Ruiz-Fresneda, M.A., Eswayah, A.S., Romero-González, M., Gardiner, P.H., Solari, P.L., Merroun, M.L., 2020. Chemical and structural characterization of Se (IV) biotransformations by *Stenotrophomonas bentonitica* into Se 0 nanostructures and volatiles Se species. Environ Sci: Nano 7 (7), 2140–2155. https://doi.org/10.1039/D0EN00507J.

[23] Lakaniemi, A.-M., Douglas, G.B., Kaksonen, A.H., 2019. Engineering and kinetic aspects of bacterial uranium reduction for the remediation of uranium contaminated environments. J Hazard Mater 371, 198–212. https://doi.org/10.1016/j.jhazmat.2019.02.074.

[24] You, W., Peng, W., Tian, Z., Zheng, M., 2021. Uranium bioremediation with U(VI)-reducing bacteria. Sci Total Environ 798, 149107. https://doi.org/10.1016/j.scitotenv.2021.149107.

[25] Povedano-Priego, C., Jroundi, F., Lopez-Fernandez, M., Sánchez-Castro, I., Martin-Sánchez, I., Huertas, F.J., et al., 2019. Shifts in bentonite bacterial community and mineralogy in response to uranium and glycerol-2-phosphate exposure. Sci Total Environ 692, 219–232. https://doi.org/10.1016/j.scitotenv.2019.07.228.

[26] Povedano-Priego, C., Jroundi, F., Lopez-Fernandez, M., Morales-Hidalgo, M., Martin-Sánchez, I., Huertas, F.J., et al., 2022. Impact of anoxic conditions, uranium (VI) and organic phosphate substrate on the biogeochemical potential of the indigenous bacterial community of bentonite. Appl Clay Sci 216, 106331. https://doi.org/10.1016/j.clay.2021.106331.

[27] Povedano-Priego, C., Jroundi, F., Solari, P.L., Guerra-Tschuschke, I., del Mar Abad-Ortega, M., Link, A., et al., 2023. Unlocking the bentonite microbial diversity and its implications in selenium bioreduction and biotransformation: advances in deep geological repositories. J Hazard Mater 445, 130557. https://doi.org/10.1016/j.jhazmat.2022.130557.

[28] Thijs, S., Op De Beeck, M., Beckers, B., Truyens, S., Stevens, V., Van Hamme, J.D., et al., 2017. Comparative evaluation of four bacteria-specific primer pairs for 16S rRNA gene surveys. Front Microbiol 8, 494. https://doi.org/10.3389/fmicb.2017.00494.

[29] Caporaso, J.G., Kuczynski, J., Stombaugh, J., Bittinger, K., Bushman, F.D., Costello, E.K., et al., 2010. QIIME allows analysis of high-throughput community sequencing data. Nat Methods 7 (5), 335–336. https://doi.org/10.1038/nmeth.f.303.

[30] Callahan, B.J., McMurdie, P.J., Rosen, M.J., Han, A.W., Johnson, A.J., Holmes, S. P., 2016. DADA2: high-resolution sample inference from Illumina amplicon data. Nat Methods 13 (7), 581–583. https://doi.org/10.1038/nmeth.3869.

[31] Robertson, C.E., Harris, J.K., Wagner, B.D., Granger, D., Browne, K., Tatem, B., et al., 2013. Explicet: graphical user interface software for metadata-driven management, analysis and visualization of microbiome data. Bioinformatics 29 (23), 3100–3101. https://doi.org/10.1093/bioinformatics/btt526.

[32] McMurdie, P.J., Holmes, S., 2013. Phyloseq: a R package for reproducible interactive analysis and graphics of microbiome census data. PLoS One 8, e61217. https://doi.org/10.1371/journal.pone.0061217.

[33] Neuwirth E. (2022). RColorBrewer: ColorBrewer Palettes. R package version 1.1–3, < ⟨https://CRAN.R-project.org/package=RColorBrewer⟩ >.

[34] R Core Team. (2022). R: A language and environment for statistical computing. R Foundation for Statistical Computing, Vienna, Austria. ⟨https://www.Rproject.org/⟩.

[35] Warnes G., Bolker B., Bonebakker L., Gentleman R., Huber W., Liaw A. et al. (2022). gplots: Various R Programming Tools for Plotting Data. R package version 3.1.3. ⟨https://CRAN.R-project.org/package=gplots⟩.

[36] Hammer, O. 2001. PAST: paleontological statistics software package for education and data analysis. Palaeontologia Electronica. ⟨http://palaeo-electronicaorg⟩.

[37] Fairley, N., Fernandez, V., Richard-Plouet, M., Guillot-Deudon, C., Walton, J., Smith, E., Flahaut, D., Greiner, M., Biesinger, M., Tougaard, S., Morgan, D., Baltrusaitis, J., 2021. Systematic and collaborative approach to problem solving using X-ray photoelectron spectroscopy. Appl Surf Sci 5, 100112. https://doi.org/10.1016/j.apsadv.2021.100112.

[40] Detman, A., Mielecki, D., Chojnacka, A., Salamon, A., Błaszczyk, M.K., Sikora, A., 2019. Cell factories converting lactate and acetate to butyrate: *Clostridium butyricum* and microbial communities from dark fermentation bioreactors. Microb Cell Factor 18 (1), 1–12. https://doi.org/10.1186/s12934-019-1085-1.

[38] Bahl, H., Andersch, W., Gottschalk, G., 1982. Continuous production of acetone and butanol by *Clostridium acetobutylicum* in a two-stage phosphate limited chemostat. Eur J Appl Microbiol Biotechnol 15, 201–205, 0171-1741/82/0015/0201/$ 01.00.

[41] Mosher, J.J., Phelps, T.J., Podar, M., Hurt Jr, R.A., Campbell, J.H., Drake, M.M., et al., 2012. Microbial community succession during lactate amendment and electron acceptor limitation reveals a predominance of metal-reducing *Pelosinus* spp. Appl Environ Microbiol 78 (7), 2082–2091. https://doi.org/10.1128/AEM.07165-11.

[39] Brockman, H.L., Wood, W.A., 1975. D-Lactate dehydrogenase of *Peptostreptococcus elsdenii.* J Bacteriol 124 (3), 1454–1461. https://doi.org/10.1128/jb.124.3.1454-1461.1975.

[42] Drot, R., Roques, J., Simoni, E., 2007. Molecular approach of the uranyl/mineral interfacial phenomena. Comptes Rendus Chim 10 (10-11), 1078–1091. https://doi.org/10.1016/j.crci.2007.01.014.

[43] Dacheux, N., Brandel, V., Genet, M., Bak, K., Berthier, C., 1996. Solid solutions of uranium and thorium phosphates: synthesis, characterization and X-ray photoelectron spectroscopy. N J Chem 20 (3), 301–310.

[44] Howng, W.Y., Thorn, R.J., 1979. X-ray photoelectron spectrum of U (4f) in condensates from UF4 and ion bombarded Uf4; spectrum of UF3. Chem Phys Lett 62 (1), 57–60. https://doi.org/10.1016/0009-2614(79)80412-1.

[45] Marin, C. (2012). Particulate Phases Possibly Conveyed from Nuclear Waste Repositories by Groundwater. INTECH Open Access Publisher.

[46] Filippidou, S., Junier, T., Wunderlin, T., Lo, C.C., Li, P.E., Chain, P.S., et al., 2015. Under-detection of endospore-forming Firmicutes in metagenomic data. Comput Struct Biotechnol J 13, 299–306. https://doi.org/10.1016/j.csbj.2015.04.002.

[47] Petriglieri, F., Nierychlo, M., Nielsen, P.H., McIlroy, S.J., 2018. In situ visualisation of the abundant *Chloroflexi* populations in full-scale anaerobic digesters and the fate of immigrating species. PLoS One 13 (11), e0206255. https://doi.org/10.1371/journal.pone.0206255.

[48] Barka, E.A., Vatsa, P., Sanchez, L., Gaveau-Vaillant, N., Jacquard, C., Klenk, H.P., et al., 2016. Taxonomy, physiology, and natural products of Actinobacteria. Microbiol Mol Biol Rev 80 (1), 1–43. https://doi.org/10.1128/mmbr.00019-15.

[49] Lopez-Fernandez, M., Matschiavelli, N., Merroun, M.L., 2021. Bentonite geomicrobiology. Microbiol Nucl Waste Dispos 137–155. https://doi.org/10.1016/B978-0-12-818695-4.00007-1.

[50] Pinel-Cabello, M., Jroundi, F., López-Fernández, M., Geffers, R., Jarek, M., Jauregui, R., et al., 2021. Multisystem combined uranium resistance mechanisms and bioremediation potential of *Stenotrophomonas bentonitica* BII-R7: transcriptomics and microscopic study. J Hazard Mater 403, 123858. https://doi.org/10.1016/j.jhazmat.2020.123858.

[51] Yu, Q., Yuan, Y., Feng, L., Sun, W., Lin, K., Zhang, J., et al., 2022. Highly efficient immobilization of environmental uranium contamination with *Pseudomonas stutzeri* by biosorption, biomineralization, and bioreduction. J Hazard Mater 424, 127758. https://doi.org/10.1016/j.jhazmat.2021.127758.

[52] Zheng, X., Hu, P., Yao, R., Cheng, J., Chang, Y., Mei, H., et al., 2022. Biosorption behavior and biomineralization mechanism of low concentration uranium(VI) by Pseudomonas fluorescens. J Radioanal Nucl Chem 331 (11), 4675–4684. https://doi.org/10.1007/s10967-022-08551-3.

[53] Chabalala, S., Chirwa, E.M., 2010. Uranium(VI) reduction and removal by high performing purified anaerobic cultures from mine soil. Chemosphere 78 (1), 52–55. https://doi.org/10.1016/j.chemosphere.2009.10.026.

[54] Choudhary, S., Sar, P., 2011. Uranium biomineralization by a metal resistant *Pseudomonas aeruginosa* strain isolated from contaminated mine waste. J Hazard Mater 186 (1), 336–343. https://doi.org/10.1016/j.jhazmat.2010.11.004.

[55] Sánchez-Castro, I., Martínez-Rodríguez, P., Jroundi, F., Solari, P.L., Descostes, M., Merroun, M.L., 2020. High-efficient microbial immobilization of solved U(VI) by the *Stenotrophomonas* strain Br8. Water Res 183, 116110. https://doi.org/10.1016/j.watres.2020.116110.

[56] Sánchez-Castro, I., Martínez-Rodríguez, P., Abad, M.M., Descostes, M., Merroun, M.L., 2021. Uranium removal from complex mining waters by alginate beads doped with cells of *Stenotrophomonas* sp. Br8: novel perspectives for metal bioremediation. J Environ Manag 296, 113411. https://doi.org/10.1016/j.jenvman.2021.113411.

[57] Sánchez-Castro, I., Ruiz-Fresneda, M.A., Bakkali, M., Kämpfer, P., Glaeser, S.P., Busse, H.J., et al., 2017. *Stenotrophomonas bentonitica* sp. nov., isolated from bentonite formations. Int J Syst Evolut Microbiol 67 (8), 2779 https://doi.org/10.1099%2Fijsem.0.002016.

[58] Engel, K., Ford, S.E., Binns, W.J., Diomidis, N., Slater, G.F., Neufeld, J.D., 2023. Stable microbial community in compacted bentonite after 5 years of exposure to natural granitic groundwater. Msphere 8 (5), e00048-23. https://doi.org/10.1128/msphere.00048-23.

[59] Fraj, B., Ben Hania, W., Postec, A., Hamdi, M., Ollivier, B., Fardeau, M.L., 2013. *Fonticella tunisiensis* gen. nov., sp. nov., isolated from a hot spring. Int J Syst Evolut Microbiol 63 (Pt_6), 1947–1950. https://doi.org/10.1099/ijs.0.041947-0.

[60] Gilmour, K.A., Davie, C.T., Gray, N., 2021. An indigenous iron-reducing microbial community from MX80 bentonite-a study in the framework of nuclear waste disposal. Appl Clay Sci 205, 106039. https://doi.org/10.1016/j.clay.2021.106039.

[61] Gilmour, K.A., Davie, C.T., Gray, N., 2022. Survival and activity of an indigenous iron-reducing microbial community from MX80 bentonite in high temperature/low water environments with relevance to a proposed method of nuclear waste disposal. Sci Total Environ 814, 152660. https://doi.org/10.1016/j.scitotenv.2021.152660.

[62] Holmes, D.E., Orelana, R., Giloteaux, L., Wang, L.Y., Shrestha, P., Williams, K., et al., 2018. Potential for *Methanosarcina* to contribute to uranium reduction during acetate-promoted groundwater bioremediation. Microb Ecol 76, 660–667. https://doi.org/10.1007/s00248-018-1165-5.

[63] Newsome, L., Morris, K., Trivedi, D., Bewsher, A., Lloyd, J.R., 2015. Biostimulation by glycerol phosphate to precipitate recalcitrant uranium(IV) phosphate. Environ Sci Technol 49 (18), 11070–11078. https://doi.org/10.1021/acs.est.5b02042.

[64] Sani, R.K., Peyton, B.M., Dohnalkova, A., 2006. Toxic effects of uranium on *Desulfovibrio desulfuricans* G20. Environ Toxicol Chem: Int J 25 (5), 1231–1238. https://doi.org/10.1897/05-401R.1.

[65] Thorgersen, M.P., Lancaster, W.A., Rajeev, L., Ge, X., Vaccaro, B.J., Poole, F.L., et al., 2017. A highly expressed high-molecular-weight S-layer complex of *Pelosinus*

sp. strain UFO1 binds uranium. Appl Environ Microbiol 83 (4), e03044-16. https://doi.org/10.1128/AEM.03044-16.
[66] Babich, T.L., Semenova, E.M., Sokolova, D.S., Tourova, T.P., Bidzhieva, S.K., Loiko, N.G., et al., 2021. Phylogenetic diversity and potential activity of bacteria and fungi in the deep subsurface horizons of an uranium deposit. Microbiology 90, 607–620. https://doi.org/10.1134/S0026261721040032.
[67] Kumari, D., Pan, X., Achal, V., Zhang, D., Al-Misned, F.A., Golam Mortuza, M., 2015. Multiple metal-resistant bacteria and fungi from acidic copper mine tailings of Xinjiang, China. Environ Earth Sci 74, 3113–3121. https://doi.org/10.1007/s12665-015-4349-z.
[68] Gupta, R.S., Patel, S., Saini, N., Chen, S., 2020. Robust demarcation of 17 distinct *Bacillus* species clades, proposed as novel Bacillaceae genera, by phylogenomics and comparative genomic analyses: description of *Robertmurraya kyonggiensis* sp. nov. and proposal for an emended genus *Bacillus* limiting it only to the members of the Subtilis and Cereus clades of species. Int J Syst Evolut Microbiol 70 (11), 5753–5798. https://doi.org/10.1099/ijsem.0.004475.
[69] Gupta, R.S., 2023. Update on the genus *Robertmurraya*: a bacterial genus honoring Dr. Robert GE Murray (with some personal reminiscences). Can J Microbiol 69 (10), 387–392. https://doi.org/10.1139/cjm-2023-0070.
[70] Banala, U.K., Das, N.P.I., Toleti, S.R., 2021. Uranium sequestration abilities of *Bacillus bacterium* isolated from an alkaline mining region. J Hazard Mater 411, 125053. https://doi.org/10.1016/j.jhazmat.2021.125053.
[71] Pan, X., Chen, Z., Chen, F., Cheng, Y., Lin, Z., Guan, X., 2015. The mechanism of uranium transformation from U(VI) into nano-uramphite by two indigenous *Bacillus thuringiensis* strains. J Hazard Mater 297, 313–319. https://doi.org/10.1016/j.jhazmat.2015.05.019.
[72] Panak, P., Raff, J., Selenska-Pobell, S., Geipel, G., Bernhard, G., Nitsche, H., 2000. Complex formation of U(VI) with *Bacillus*-isolates from a uranium mining waste pile. Radiochim Acta 88 (2), 71–76. https://doi.org/10.1524/ract.2000.88.2.071.
[73] Chang, Y.J., Peacock, A.D., Long, P.E., Stephen, J.R., McKinley, J.P., Macnaughton, S.J., et al., 2001. Diversity and characterization of sulfate-reducing bacteria in groundwater at a uranium mill tailings site. Appl Environ Microbiol 67 (7), 3149–3160. https://doi.org/10.1128/AEM.67.7.3149-3160.2001.
[74] Zhu, F., Zhao, B., Min, W., Li, J., 2023. Characteristics of groundwater microbial communities and the correlation with the environmental factors in a decommissioned acid in-situ uranium mine. Front Microbiol 13, 1078393. https://doi.org/10.3389/fmicb.2022.1078393.
[75] Lee, G., Lee, W., 2021. Adsorption of uranium from groundwater using heated aluminum oxide particles. J Water Process Eng 40, 101790. https://doi.org/10.1016/j.jwpe.2020.101790.
[76] Wazne, M., Korfiatis, G.P., Meng, X., 2003. Carbonate effects on hexavalent uranium adsorption by iron oxyhydroxide. Environ Sci Technol 37 (16), 3619–3624. https://doi.org/10.1021/es034166m.
[77] Latta, D.E., Boyanov, M.I., Kemner, K.M., O'Loughlin, E.J., Scherer, M.M., 2012. Abiotic reduction of uranium by Fe(II) in soil. Appl Geochem 27 (8), 1512–1524. https://doi.org/10.1016/j.apgeochem.2012.03.003.
[78] Wang, Q., Zhu, C., Huang, X., Yang, G., 2019. Abiotic reduction of uranium(VI) with humic acid at mineral surfaces: competing mechanisms, ligand and substituent effects, and electronic structure and vibrational properties. Environ Pollut 254, 113110. https://doi.org/10.1016/j.envpol.2019.113110.
[79] Tsarev, S., Waite, T.D., Collins, R.N., 2016. Uranium reduction by Fe(II) in the presence of montmorillonite and nontronite. Environ Sci Technol 50 (15), 8223–8230. https://doi.org/10.1021/acs.est.6b02000.
[80] Boonchayaanant, B., Gu, B., Wang, W., Ortiz, M.E., Criddle, C.S., 2010. Can microbially-generated hydrogen sulfide account for the rates of U(VI) reduction by a sulfate-reducing bacterium? Biodegradation 21, 81–95. https://doi.org/10.1007/s10532-009-9283-x.
[81] Beazley, M.J., Martinez, R.J., Sobecky, P.A., Webb, S.M., Taillefert, M., 2007. Uranium biomineralization as a result of bacterial phosphatase activity: insights from bacterial isolates from a contaminated subsurface. Environ Sci Technol 41 (16), 5701–5707. https://doi.org/10.1021/es070567g.
[82] Krivovichev, S.V., Burns, P.C., Tananaev, I.G., 2006. Crystal chemistry of actinide phosphates and arsenates. Struct Chem Inorg Actin Compd 217.
[83] Hufton, J., Harding, J., Smith, T., Romero-González, M.E., 2021. The importance of the bacterial cell wall in uranium(VI) biosorption. Phys Chem Chem Phys 23 (2), 1566–1576. https://doi.org/10.1039/D0CP04067C.
[84] Alessi, D.S., Lezama-Pacheco, J.S., Stubbs, J.E., Janousch, M., Bargar, J.R., Persson, P., et al., 2014. The product of microbial uranium reduction includes multiple species with U(IV)–phosphate coordination. Geochim Et Cosmochim Acta 131, 115–127. https://doi.org/10.1016/j.gca.2014.01.005.
[85] McLean, J., Beveridge, T.J., 2001. Chromate reduction by a pseudomonad isolated from a site contaminated with chromated copper arsenate. Appl Environ Microbiol 67 (3), 1076–1084. https://doi.org/10.1128/AEM.67.3.1076-1084.2001.
[86] Sani, R.K., Peyton, B.M., & Dohnalkova, A. (2004). Effect of uranium(VI) on Desulfovibrio desulfuricans G20: influence of soil minerals. 104th General Meeting of the Asm (Abstract).